An efficient direct BEM numerical scheme for heat transfer problems using Fourier series

Maria T. Ibáñez and H. Power
Wessex Institute of Technology, Southampton, UK, and Facultad de Ingeniería, Universidad Central de Venezuela, Venezuela

Received November 1999
Revised July 2000
Accepted July 2000

Keywords *Boundary element method, Heat transfer, Numerical solutions*

Abstract *The main objective is to develop an efficient BEM scheme for the numerical solution of two-dimensional heat problems. Our scheme will be of the re-initialization type, in which the domain integrals are computed by a recursion relation which depends only on the boundary temperature and flux at previous time step. To obtain the re-initialization approach, we will use in the integral representation formula a Green function corresponding to zero temperature in a box containing the original domain, instead of using the classical free space fundamental solution. This Green function is given in terms of the original fundamental solution plus a regular solution of the heat equation inside the domain under consideration. It can therefore be used in the integral representation formula of the heat equation (direct formulation) to obtain the solution of a heat problem in such a domain. The Green function mentioned can be obtained by the images method, and the resulting source series can also be rewritten in terms of a double Fourier series, that we will use in the domain integral of the integral representation formula to transform such integral into equivalent surface integrals.*

1. Introduction

The boundary element method (BEM) is a numerical method for the solution of boundary integral equations, based on a discretization procedure. Nowadays, it is an important alternative to the prevailing domain methods of analysis in continuum mechanics, such as finite differences (FDM) or finite elements (FEM).

The basis of the method is to transform the original partial differential equation (PDE), or system of PDEs, that define a given physical problem into an equivalent integral equation (or system) by means of the corresponding Green's representation formula (direct method), or in terms of continuous distribution of singular solutions of the PDE over the boundaries of the problem (indirect method). The unknowns in the integral formulation of the boundary value problem would be either the primitive variables on the boundary (direct formulation) or fictitious surface densities of the singular solutions (indirect formulation). In this way, the integral equation obtained satisfies the governing field equation exactly, and one seeks to satisfy the imposed boundary conditions approximately.

The Green's integral representation formula for the heat equation, which is of the Volterra-Fredholm type, has been extensively used in the literature and

The authors would like to express their appreciation to the referees for their useful comments.

its formulation can be traced back to the works of Morse and Feshbach (1953), and Carslaw and Jaeger (1959). Chang *et al.* (1973) and Shaw (1974) were the first to apply this formulation in the context of the direct BEM numerical technique (see also Wrobel and Brebbia (1979)). The indirect formulation in terms of a single or a double layer potential is less popular; however, this approach has also been successfully implemented in the past. The uniqueness of solution of each of the resulting integral equations for both approaches, i.e. direct and indirect, when applied to solve Dirichlet, Neumann or mixed initial boundary value problems has been proved by Hsiao and Saranen (1993). This uniqueness of solution follows from the good behaviour of Volterra integral equations of the first or second kind with bounded kernel, for which a unique continuous solution always exists. This is not necessarily the case when dealing with only Fredholm equations.

Two alternative approaches have been adopted in the literature for the implementation of the time stepping integration of the direct BEM formulation (for more details see Brebbia *et al.* (1984)). One of these involves the re-initiation at each time step, which presents the problem of repeated domain integral evaluation at each time step. The other time stepping approach is the convolution method which involves integrating back to the initial time. This technique makes use of the simplicity of the initial conditions to avoid the need for domain integration. These two approaches become impractical after a number of time steps. In the first case, due to the number of domain integrals required and, in the second, due to the requirement of the evaluation of the history-dependence, representing more and more work as time proceeds. Consequently, by using these two classical approaches, the evaluation of the temperature field requires more and more computational work as time progresses.

In order to overcome these difficulties, Demirel and Wang (1987) developed a truncation algorithm to improve the computational efficiency of the convolution method, by computing only approximately the influence of initial steps after some time had elapsed, i.e. they divided the whole integral into near-history and far-history integrals, where the near-history is evaluated in the normal procedure while the far-history one is computed using a truncation approximation, due to the fact that the fundamental solution decays with time. Davey and Hinduja (1987) proposed an approximate transformation of the domain integrals to the boundary by representing the fundamental solution in terms of a linear superposition of finite number of heat sources positioned at different points in time (see also Davey and Bounds, 1996; Singh and Kalra, 1995), followed the same idea of transforming the domain integral to the boundary, but used the dual reciprocity approximation. More recently Zerroukat (1998) proposed an algorithm which combines the BEM and a scheme which uses virtual collocation points and radial basis functions to approximate the domain integral (see also Zerroukat *et al.*, 1998; Zerroukat and Power, 1998). It is important to mention that the works by Davey and Bounds

(1996) and Zerroukat (1998) have several similarities to and differences from the present work, that are worthy of special attention. In section 6 we analyse these common and different features between these works.

Similar difficulties to the ones presented with the time stepping integration of the direct BEM formulation are encountered when the problem is solved by an indirect formulation. Greengard and Strain (1990) proposed an indirect formulation for Dirichlet initial boundary value problems based on a single layer representation alone that avoids the history-dependence of the time integration of the single layer potential (see also Sethian and Strain, 1992; Strain, 1992). Greengard and Strain's (1990) single layer formulation is of the convolution type, in which the time integration is sub-divided into two intervals, from zero to $T - \delta$ and from $T - \delta$ to T, with a very small value of δ. Instead of using the free space fundamental solution as the kernel of the single layer potential, they use the Dirichlet Green function in a rectangular box that contains the original problem domain Ω (see Figure 1). Therefore, such Green function is a regular solution of the heat equation at any point interior to the box except at the singular point, i.e. at $\vec{x} = \vec{z}$ as $t \to T$, having zero value at the box contour. The general expression of such Green function is found in terms of an infinite series of heat sources (images method). The Fourier series representation of this infinite series of heat sources is known as the bilinear formula of the Green function (Carslaw and Jaeger, 1959).

Greengard and Strain (1990) showed that the infinite series of heat sources converges exponentially fast for values of t near to the evaluation time T, whereas its Fourier series representation also converges exponentially fast but for values of t not too near to T. Therefore, they used the Fourier series representation of the Green function as the kernel of the single layer on the time interval from zero to $T - \delta$, and the infinite series of sources on the time interval

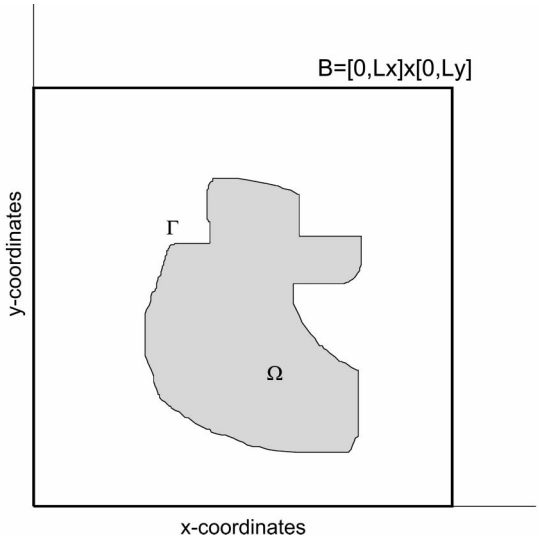

Figure 1.
Domain Ω contained in the box B. Γ is the boundary of Ω

$T - \delta$ to T. For small value of δ, they proved that using only the leading term in the series of sources, i.e. the free space fundamental solution, also yields to an exponentially small truncation error on the evaluation of the integral of the single layer potential over the time integral $T - \delta$ to T.

By interchanging integration and summation operators on the interval from zero to $T - \delta$, which can be carried out formally due to the uniform convergence of a Fourier series (see Tolstov, 1962), it is possible to express this part of the single layer as a uniform convergent Fourier series, which Fourier coefficients can be obtained recursively in terms of the coefficients of the series at previous time intervals, plus some surface integrals of trigonometric moments at the time interval in consideration. With this approach it is possible to evaluate efficiently the history-dependence of the indirect single layer integral equation formulation (convolution type) with Dirichlet boundary condition.

The main objective of our work is to extend Greengard and Strain (1990) single layer indirect integral equation formulation of the convolution type for the heat equation with Dirichlet boundary condition to the direct integral equation formulation of the re-initialization type, which besides having a single layer potential also involves a double layer potential. The use of the direct formulation is justified by the versatility of the approach to deal with different types of boundary conditions, in particular with mixed boundary conditions.

By using the Fourier series representation of the above Green function as the kernel of the single layer potential, and the normal derivative of the series as the kernel of the double layer potential, we are able to prove that the domain integral at the time $T - \Delta t$ of the re-initialization approach can be written as a uniform convergent Fourier series, which truncation error can be estimated from the residual of the series resulting in an exponentially small value (see Appendix 1). As in the case of the Greengard and Strain (1990) approach, in our case the Fourier coefficients can be obtained recursively in terms of the coefficients of the series of the previous time step plus some surface integrals of trigonometric moments at the time of evaluation of the domain integral.

In first instance, the evaluation of our single and double layer surface potentials at the time interval $T - \Delta T$ to T is approximated by using the leading terms of the source series representation of the Green function and its normal derivative, i.e. the free space fundamental solution and its normal derivative, as suggested by Greengard and Strain (1990) for the single layer potential alone. The estimation of the truncation error for both potentials shows exponential small value for small Δt. Having found the estimation of the truncation errors in the evaluation of the single and double layer surface potentials, it was possible to evaluate how much improvement in the accuracy of the solution for large values of Δt can be gained by adding further images (sources) to the truncated representation of the Green function. In this way, it was possible to prove that for large values of Δt significant improvement in the solution can be obtained without changing the computational complexity of the algorithm. Since with this change we are only required to evaluate more

complex forms of the kernels of the single and double layer potentials (with the same order of singularities), and therefore no additional computational complexity is introduced.

Although it is possible to prove that a similar approach to the one developed in this article can be obtained for the case of 3D problems. For simplicity of numerical implementation, we decided to carry out all our analysis and examples for 2D problems, as was also the case in the Greengard and Strain papers.

2. Boundary integral equation

The thermal diffusion problem in absence of sources in the domain Ω is governed by the parabolic equation

$$\alpha \bigtriangledown^2 u(\vec{z}, t) = \frac{\partial u(\vec{z}, t)}{\partial t}, \qquad \forall \vec{z} \in \Omega \tag{1}$$

where Ω is a two-dimensional bounded domain, contained in the box $B = [0, L_x] \times [0, L_y]$, and bounded by closed curve Γ, u represents the temperature, t the time and α the thermal diffusivity, which is considered here to be constant.

This equation can be transformed into the following familiar boundary integral representation (convolution formulation):

$$\begin{aligned} u(\vec{z}, T) &= \alpha \int_0^T \int_\Gamma u^*(\vec{z}, \vec{x}, T, t) q(\vec{x}, t) d\Gamma_{\vec{x}} dt \\ -\alpha \int_0^T \int_\Gamma q^*(\vec{z}, \vec{x}, T, t) u(\vec{x}, t) d\Gamma_{\vec{x}} dt &+ \int_\Omega u_0(\vec{x}, t_0) u^*(\vec{z}, \vec{x}, T, t_0) d\Omega_{\vec{x}} \end{aligned} \tag{2}$$

for every $\vec{z} \in \Omega \subset B = [0, L_x] \times [0, L_y]$, which provides the exact value of u at a point $\vec{z}$ inside the domain Ω, at a time T once the boundary values of u, $q = \frac{\partial u}{\partial n_{\vec{x}}}$ and the initial condition $u_0(\vec{x}, t_0)$ are all known , where $n_{\vec{x}} = (n_{\vec{x}_1}, n_{\vec{x}_2})$ is the unit outward normal to the boundary Γ.

In the above equation the first term is known as the single layer potential with the fundamental solution of the heat equation, i.e.

$$u^*(\vec{z}, \vec{x}, T, t) = \frac{1}{4\pi\alpha(T-t)} \exp\{- \| \vec{z} - \vec{x} \|^2 / 4\alpha(T-t)\} \tag{3}$$

as its kernel and the normal derivative of the temperature field at the surface Γ, as its density, i.e. q. The second term is the double layer potential with the normal derivative of the fundamental solution, $q^* = \frac{\partial u^*}{\partial n_{\vec{x}}}$, as its kernel and the temperature field u, at the surface Γ as its density. The last integral term is the volume potential with the fundamental solution as its kernel and the initial temperature field at Ω as its density.

The main difficulty encountered with the numerical evaluation of the above integral representation formula lies in the coupled behaviour between the

independent variables $\vec{z}$ (collocation point in space), $\vec{x}$ (integration point in space), T (collocation point in time or evaluation time) and t (integration point in time), of the integration kernels. This coupling forces the integral of the single and double layer at each element to be evaluated n times at each time interval, with n equal to the number of collocation points which is at least equal to the number of elements N (in the case of constant element). These integrations have to be repeated every time the evaluation time is changed (history-dependence).

As mentioned in the introduction, in order to avoid the evaluation of these integrals at every time step, $t = t_l$, the re-initiation approach treats each time step as a new problem where the value of the temperature field at the previous time step is used as the initial condition. In this way in the re-initialization BEM scheme, the temperature field, at any point inside the domain Ω, is given by the following integral representation formula:

$$\begin{aligned} u(\vec{z}, t_l) = \alpha \int_{t_l-\Delta t}^{t_l} \int_{\Gamma} u^*(\vec{z}, \vec{x}, t_l, t) q(\vec{x}, t) d\Gamma_{\vec{x}} dt \\ -\alpha \int_{t_l-\Delta t}^{t_l} \int_{\Gamma} q^*(\vec{z}, \vec{x}, t_l, t) u(\vec{x}, t) d\Gamma_{\vec{x}} dt \\ + \int_{\Omega} u(\vec{x}, t_l - \Delta t) u^*(\vec{z}, \vec{x}, t_l, t_l - \Delta t) d\Omega_{\vec{x}} \end{aligned} \tag{4}$$

where $t_l = l\Delta t$, $l = 1, 2, \ldots, M$. The final evaluation time is achieved at $M\Delta t$, i.e. $T = M\Delta t$.

By defining the change of variable $\tau = t - (t_l - \Delta)t$, the above formula can be rewritten as:

$$\begin{aligned} u(\vec{z}, t_l) = \alpha \int_{0}^{\Delta t} \int_{\Gamma} u^*(\vec{z}, \vec{x}, \Delta t, \tau) q(\vec{x}, \tau + t_l - \Delta t) d\Gamma_{\vec{x}} d\tau - \\ \alpha \int_{0}^{\Delta t} \int_{\Gamma} q^*(\vec{z}, \vec{x}, \Delta t, \tau) u(\vec{x}, \tau + t_l - \Delta t) d\Gamma_{\vec{x}} d\tau \\ + \int_{\Omega} u(\vec{x}, t_l - \Delta t) u^*(\vec{z}, \vec{x}, \Delta t, 0) d\Omega_{\vec{x}} \end{aligned} \tag{5}$$

where $u^*(\vec{z}, \vec{x}, t_l, t_l - \Delta t) = u^*(\vec{z}, \vec{x}, \Delta t, 0)$.

The main difficulty in the implementation of this scheme consists of the domain integration of the pseudo-initial value $u(\vec{x}, t_l - \Delta t)$ at each time step. With the present approach these domain integrals can be obtained in a recursively manner in terms of only surface integrals that are independent of the number of collocation points. As we will comment in Section 6, this is one of the main features that make our approach different from other alternative approaches previously reported in the literature.

Instead of using the classical free space fundamental solution, u^* (heat source), and its normal derivative, q^*, as the kernels of the above integral representation formula, in this work we will use the following Green function, $G(\vec{z}, \vec{x}, T, t)$, that consists of a series of heat sources:

$$G(\vec{z},\vec{x},T,t) = \frac{1}{4\pi\alpha(T-t)} \sum_{\substack{n_1=-\infty \\ n_2=-\infty}}^{\infty} \sum_{\substack{\sigma_1=\pm 1 \\ \sigma_2=\pm 1}}^{\infty} \sigma_1\sigma_2 \exp\left\{ -\frac{\|\vec{z} - \sigma \cdot \vec{x} - 2nL\|^2}{4\alpha(T-t)} \right\} \quad (6)$$

where $\sigma \cdot \vec{x} = (\sigma_1 x_1, \sigma_2 x_2)$, $2nL = (2n_1 L_x, 2n_2 L_y)$, with its corresponding normal flux

$$Q(\vec{z},\vec{x},T,t) = \frac{\partial G(\vec{z},\vec{x},T,t)}{\partial \vec{n}_{\vec{x}}}$$

The above Green function is obtained by the images method and it corresponds to the fundamental solution of the heat equation in the box B with zero Dirichlet boundary conditions on the box walls ∂B (see Figure 2). As can be observed, equation (6) is given in terms of the original free space fundamental solution inside the box B, i.e. the term $n_1 = n_2 = 0$, $\sigma_{1,2} = 1$, plus a series that represents a regular solution of the heat equation at every $\vec{x} \in \bar{B}$. It can therefore be used directly in the above integral representation formula, i.e. equation (1) or equation (5).

It is important to observe that in the present case the use of a Green function is not with the objective of avoiding one of the integrals (or part of it) in the

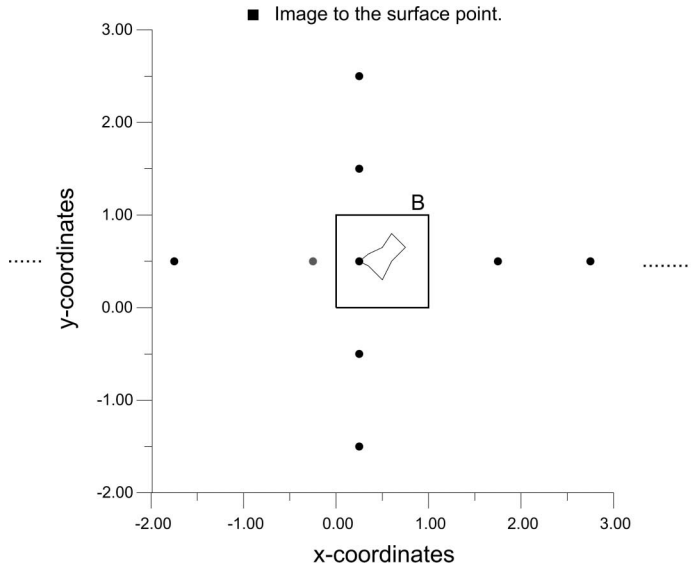

Figure 2.
Image system for one point on the surface

integral representation formula, but with the idea of having an efficient way of evaluating the corresponding domain integrals of the re-initialization BEM scheme, as we will see later.

The above Green function has an equivalent representation in terms of Fourier series (Dym and McKean, 1972), which is given by:

$$K(\vec{z},\vec{x},T,t)=\frac{4}{L_xL_y}\sum_{\substack{k_1=1\\k_2=1}}^{\infty}e^{-\pi^2k^2\alpha(T-t)}\sin\frac{\pi k_1x_1}{L_x}\sin\frac{\pi k_2x_2}{L_y}\sin\frac{\pi k_1z_1}{L_x}\sin\frac{\pi k_2z_2}{L_y} \quad (7)$$

where $k^2=\frac{k_1^2}{L_x^2}+\frac{k_2^2}{L_y^2}$ and L_x, L_y are the dimensions of the box B.

It is important to notice that, in the series representation of the Green function, the independent variables $\vec{z}$, $\vec{x}$, T, and t are completely uncoupled. In the classical mathematical theory of integral equations, the truncated form of this type of Fourier series representation of the integral kernel is used to reduce the original integral equation to an equation with degenerate kernel, which solution can be exactly transformed to the solution of a linear algebraic system of equation. General existence and uniqueness theorems can be obtained using this type of analysis (Mikhlin, 1957). From the computational point of view this approach is impractical due to the low rate of convergence of the above series for values of t close to T.

As Greengard and Strain (1990) pointed out, the Green function given in terms of its Fourier expansion converges exponentially fast for values of t not too close to T. Therefore, in our new re-initiation scheme, this Fourier series will be used to evaluate the domain integrals.

On the other hand, the convergence of the original Green function is also exponentially fast when $(T - t)$ is small, if it is expressed by means of the representation derived from the images method, $G(\vec{z}, \vec{x}, T, t)$, which makes its use suitable for the definition of the single and double layer kernels in equation (5). In this way equation (5) can be written as:

$$\begin{aligned}u(\vec{z},t_l)=&\alpha\int_0^{\Delta t}\int_\Gamma G(\vec{z},\vec{x},\Delta t,\tau)q(\vec{x},\tau+t_l-\Delta t)d\Gamma_{\vec{x}}d\tau\\&-\alpha\int_0^{\Delta t}\int_\Gamma Q(\vec{z},\vec{x},\Delta t,\tau)u(\vec{x},\tau+t_l-\Delta t)d\Gamma_{\vec{x}}d\tau\\&+\int_\Omega u(\vec{x},t_l-\Delta t)K(\vec{z},\vec{x},\Delta t,0)d\Omega_{\vec{x}}\end{aligned} \quad (8)$$

In order to evaluate the domain integrals in the above Green's integral representational formula, let us consider the temperature field at a time t', $0 < t' \leqslant T$, given in terms of the convolution formula equation (2) with the Fourier series representation $K(\vec{z},\vec{x},t',t)$ of the Green function and its normal derivative as the kernels of the single and double layer potentials, respectively, i.e.

$$u(\vec{z},t') = \alpha \int_0^{t'} \int_\Gamma K(\vec{z},\vec{x},t',t) q(\vec{x},t) d\Gamma_{\vec{x}} dt - \alpha \int_0^{t'} \int_\Gamma \frac{\partial K(\vec{z},\vec{x},t',t)}{\partial n_{\vec{x}}} u(\vec{x},t) d\Gamma_{\vec{x}} dt \tag{9}$$

where for simplicity, we assumed that the initial temperature is zero, resulting in an initial zero domain integral. Further comments on the general case of non-zero initial condition will be given at the end of the next section.

In fact, the use of the Green function, on the Green integral representation formula allows us to obtain, at each time t', an expression $D(\vec{z}, t')$, for every $\vec{z} \in B$, which will be equal to the temperature field $u(\vec{z}, t')$ inside Ω, equal to zero value in the domain exterior to Ω, bounded by ∂B and Γ, and whose limiting value at a point $\vec{\xi}$ on the boundary Γ is equal to $c\left(\vec{\xi}\right) u\left(\vec{\xi}, t'\right)$, where $c\left(\vec{\xi}\right)$ represents the solid angle at a source point and it can be taken as equal to $\frac{1}{2}$ if Γ is smooth, i.e.

$$D(\vec{z},t') = \begin{cases} u(\vec{z},t') & \text{if } \vec{z} \in \Omega \\ \frac{1}{2} u(\vec{z},t') & \text{if } \vec{z} \in \Gamma \\ 0 & \text{if } \vec{z} \in B - \bar{\Omega} \end{cases} \tag{10}$$

The double Fourier series representation of this discontinuous function, at the time t', is given by:

$$D(\vec{z},t') = \frac{4}{L_x L_y} \sum_{k_3=1}^{\infty} \sum_{k_4=1}^{\infty} I_{k_3 k_4}(t') \sin \pi \frac{k_3}{L_x} z_1 \sin \pi \frac{k_4}{L_y} z_2, \quad \vec{z} \in B \tag{11}$$

whose coefficients are defined by:

$$I_{k_3 k_4}(t') = \int_B D(\vec{z},t') \sin \pi \frac{k_3}{L_x} z_1 \sin \pi = \frac{k_4}{L_y} z_2 d\Omega_{\vec{z}} = \int_\Omega u(\vec{z},t') \sin \pi \frac{k_3}{L_x} z_1 \sin \pi \frac{k_4}{L_y} z_2 d\Omega_{\vec{z}} \tag{12}$$

where the reduction of the domain integration over the rectangular box B to the integration over the domain Ω is due to the discontinuous behaviour given by equation (10), in which the function $u(\vec{z}, t')$ is given by equation (9) with the double Fourier series equation (7) and its normal derivative as the kernels of the corresponding single and double layer potentials.

To proceed with this evaluation, we begin by denoting $u_{k_1 k_2}(t)$ and $q_{k_1 k_2}(t)$ as the space integrals, i.e.

$$u_{k_1k_2}(t) = \int_\Gamma \frac{\partial\left(\sin\pi\frac{k_1}{L_x}x_1 \sin\pi\frac{k_2}{L_y}x_2\right)}{\partial n_{\vec{x}}} u(\vec{x},t)d\Gamma_{\vec{x}},$$

and

$$q_{k_1k_2}(t) = \int_\Gamma \sin\pi\frac{k_1}{L_x}x_1 \sin\pi\frac{k_2}{L_y}x_2 q(\vec{x},t)d\Gamma_{\vec{x}}$$

which are defined by Greengard and Strain (1990) as the surface trigonometric moments of u and q, respectively. Owing to the uncoupled behaviour of the independent variables $\vec{z}$, $\vec{x}$, t' and t of the new kernels, these moment coefficients are independent of the collocation points and the final time of evaluation. In this way, equation (9) can be rewritten as:

$$u(\vec{z},t') = \frac{4\alpha}{L_xL_y}\sum_{\substack{k_1=1\\k_2=1}}^{\infty}\left\{\int_0^{t'} e^{-\pi^2\alpha\left(\frac{k_1^2}{L_x^2}+\frac{k_2^2}{L_y^2}\right)(t'-t)} q_{k_1k_2}(t)dt\right\}\cdot \sin\frac{\pi k_1 z_1}{L_x}\sin\frac{\pi k_2 z_2}{L_y}$$
$$-\frac{4\alpha}{L_xL_y}\sum_{\substack{k_1=1\\k_2=1}}^{\infty}\left\{\int_0^{t'} e^{-\pi^2\alpha\left(\frac{k_1^2}{L_x^2}+\frac{k_2^2}{L_y^2}\right)(t'-t)} u_{k_1k_2}(t)dt\right\}\cdot \sin\frac{\pi k_1 z_1}{L_x}\sin\frac{\pi k_2 z_2}{L_y} \quad (13)$$

$\forall\vec{z}\in\Omega$

The manipulation of integral/summation operators of the above single layer potential is identical to the one carried out by Greengard and Strain (1990). However, similar analysis is required for the double layer potential that appears in the direct formulation. The interchange of integral/summation operators of the double layer potential can be guaranteed, since at every point inside the box except at the singular point the Green function is a regular solution of the heat equation having a well defined directional derivative. Therefore, according to the Fourier series theory, the derivative of the series representation of the Green function at those points is also a uniform convergent Fourier series representing the derivative of the original function (see Tolstov, 1962). The condition of uniform convergence is enough to guarantee the above operation interchange and the convergence of the resulting series.

Now, substituting the above expression for $u(\vec{z}, t')$ in the previous equation for the Fourier coefficients of the function $D(\vec{z}, t')$, i.e. equation (12), and using the orthogonal property of the set $\left\{\sin\pi\frac{k_1}{L_x}z_1 \sin\pi\frac{k_2}{L_y}z_2\right\}_{k_1,k_2=1}^{\infty}$ on the rectangle $[0, L_x]\times[0, L_y]$, we obtain

$$I_{k_3k_4}(t') = \alpha \int_0^{t'} e^{-\pi^2\alpha\left(\frac{k_3^2}{L_x^2}+\frac{k_4^2}{L_y^2}\right)(t'-t)} \left(q_{k_3k_4}(t) - u_{k_3k_4}(t)\right) dt \tag{14}$$

By splitting the time integration into two intervals $[0, t' - \Delta t]$ and $[t' - \Delta t, t']$, the above coefficients can be written as

$$\begin{aligned} I_{k_3k_4}(t') &= e^{-\pi^2\alpha\left(\frac{k_3^2}{L_x^2}+\frac{k_4^2}{L_y^2}\right)\Delta t} I_{k_3k_4}(t' - \Delta t) \\ &+\alpha \int_{t'-\Delta t}^{t'} e^{-\pi^2\alpha\left(\frac{k_3^2}{L_x^2}+\frac{k_4^2}{L_y^2}\right)(t'-t)} \left(q_{k_3k_4}(t) - u_{k_3k_4}(t)\right) dt \end{aligned} \tag{15}$$

Using a linear interpolation for $u_{k_3k_4}(t)$ and $q_{k_3k_4}(t)$, which implies that u and q vary linearly in time and integrating analytically, it is possible to obtain the following recursion relation:

$$\begin{aligned} I_{k_3k_4}(t') &= e^{-\pi^2\alpha\left(\frac{k_3^2}{L_x^2}+\frac{k_4^2}{L_y^2}\right)\Delta t} I_{k_3k_4}(t' - \Delta t) \\ &+\left(\frac{1}{\pi^2\left(\frac{k_3^2}{L_x^2}+\frac{k_4^2}{L_y^2}\right)}\right)\left[1 - \left(\frac{1 - e^{-\pi^2\alpha\left(\frac{k_3^2}{L_x^2}+\frac{k_4^2}{L_y^2}\right)\Delta t}}{\pi^2\alpha\left(\frac{k_3^2}{L_x^2}+\frac{k_4^2}{L_y^2}\right)\Delta t}\right)\right]\left(q_{k_3k_4}(t') - u_{k_3k_4}(t')\right) + \\ &-\left(\frac{1}{\pi^2\left(\frac{k_3^2}{L_x^2}+\frac{k_4^2}{L_y^2}\right)}\right)\left[e^{-\pi^2\alpha\left(\frac{k_3^2}{L_x^2}+\frac{k_4^2}{L_y^2}\right)\Delta t} - \left(\frac{1 - e^{-\pi^2\alpha\left(\frac{k_3^2}{L_x^2}+\frac{k_4^2}{L_y^2}\right)\Delta t}}{\pi^2\alpha\left(\frac{k_3^2}{L_x^2}+\frac{k_4^2}{L_y^2}\right)\Delta t}\right)\right] \cdot \\ &\cdot\left(q_{k_3k_4}(t' - \Delta t) - u_{k_3k_4}(t' - \Delta t)\right), \end{aligned} \tag{16}$$

which only depends on the boundary values of u and q at the times t' and $t' - \Delta t$, and the value of the coefficients at the previous time step. In this work we also use linear interpolation for the space variation of the temperature u, and flux q, in order to obtain the values of the functions $u_{k_3k_4}(t')$ and $q_{k_3k_4}(t')$. In this case, the integrations can be carried out analytically (see Appendix 2), where the functions to be integrated are products of polynomials of order one by sine and cosine functions, which depend on neither the time nor the collocation point and can be defined in terms of their nodal values, exclusively. Therefore, they are calculated only once in the whole process.

Considering $u(\vec{x}, 0) = 0$, it follows that $I_{k_3k_4}(0) = 0$ is the starting point in the recursion relation, to the first time step. Thus, each coefficient $I_{k_3k_4}$ can be updated with constant work per time step, rather than recomputed from $t = 0$.

Now coming back to evaluate the domain integral in our re-initialization scheme, using the Green function in terms of its Fourier series, i.e. equation (7), we can write:

$$\begin{aligned}&\int_\Omega K(\vec{z},\vec{x},\Delta t,0)u(\vec{x},t_l-\Delta t)d\Omega_{\vec{x}}\\ &=\frac{4}{L_xL_y}\sum_{k_1,k_2=1}^{\infty}e^{-\pi^2k^2\alpha\Delta t}\left\{\int_\Omega u(\vec{x},t_l-\Delta t)\sin\pi\frac{k_1}{L_x}x_1\sin\pi\frac{k_2}{L_y}x_2dx_1dx_2\right\}\cdot\\ &\qquad\cdot\sin\pi\frac{k_1}{L_x}z_1\sin\pi\frac{k_2}{L_y}z_2\end{aligned}\tag{17}$$

From our previous analysis it follows that the domain integrals of the right-hand side of the above expression are equal to the Fourier coefficients, $I_{k_1k_2}(t_l - \Delta t)$, of the series representation of the temperature field at $t' = t_l - \Delta t$ (see equation (12)); consequently we have

$$\begin{aligned}&\int_\Omega K(\vec{z},\vec{x},\Delta t,0)u(\vec{x},t_l-\Delta t)d\Omega_{\vec{x}}\\ &=\frac{4}{L_xL_y}\sum_{k_1=1}^{\infty}\sum_{k_2=1}^{\infty}e^{-\pi^2k^2\alpha\Delta t}I_{k_1k_2}(t_l-\Delta t)\sin\pi\frac{k_1}{L_x}z_1\sin\pi\frac{k_2}{L_y}z_2\end{aligned}\tag{18}$$

In this way, our re-initiation integral representation formula can be given by:

$$\begin{aligned}u(\vec{z},t_l)&=\alpha\int_0^{\Delta t}\int_\Gamma G(\vec{z},\vec{x},\Delta t,\tau)q(\vec{x},\tau+(t_l-\Delta t))d\Gamma_{\vec{x}}d\tau\\ &-\alpha\int_0^{\Delta t}\int_\Gamma Q(\vec{z},\vec{x},\Delta t,\tau)u(\vec{x},\tau+(t_l-\Delta t))d\Gamma_{\vec{x}}d\tau\\ &+\frac{4}{L_xL_y}\sum_{k_1=1}^{\infty}\sum_{k_2=1}^{\infty}e^{-\pi^2k^2\alpha\Delta t}I_{k_1k_2}(t_l-\Delta t)\sin\pi\frac{k_1}{L_x}z_1\sin\pi\frac{k_2}{L_y}z_2\end{aligned}\tag{19}$$

for $l = 1, 2, \ldots, M$, where the Fourier coefficients $I_{k_1k_2}(t_l - \Delta t)$ are obtained in a recursive manner from equation (16) with $t' = t_l - \Delta t$.

The convergence of the above trigonometric series follows directly from the comparison test of the first kind (see Knopp, 1956), since each of its terms is smaller, in absolute value, than those of the corresponding Fourier series obtained when Δt is equal to zero, i.e. equation (11). Although the above equation can be obtained by applying Greengard and Strain's (1990) decomposition scheme for a single layer potential, to the single and double layer potentials that appear on the convolution integral representational

formula given by equation (2), it is our opinion that the proposed approach is more natural and robust, in particular on the analysis of the convergence of the obtained series due to the use of the Fourier theory.

Also it is relevant to emphasize that changing the time step in the new scheme does not represent an increasing of the CPU-time because that change is only present in the factor

$$e^{-\pi^2\left(\frac{k_1^2}{L_x^2}+\frac{k_2^2}{L_y^2}\right)\alpha\Delta t}$$

in the double series which represents the domain integral. On the other hand, any change in the time step in the classical re-initialization scheme involves revaluation of the domain integral, due to the form of the fundamental solution.

3. Proposed numerical scheme

Our approach is based on the numerical solution of the integral equation obtained when the integral representation formula equation (19) is evaluated at a collocation point $\vec{\xi}$ on the surface Γ, after substituting the boundary conditions of the problem in the corresponding surface potentials.

In first order of approximation, for small values of Δt, the images series $G(\vec{z}, \vec{x}, \Delta t, \tau)$ can be given by the free-space fundamental solution $u^*(\vec{z}, \vec{x}, \Delta t, \tau)$. Indeed, u^* is the leading term of G with $\sigma_i = 1$, $i = 1, 2$ and $\vec{m} = \vec{0}$. The remainder of the series has exponential decay, i.e.

$$| G(\vec{z}, \vec{x}, \Delta t, \tau) - u^*(\vec{z}, \vec{x}, \Delta t, \tau) | = O\left(\frac{\exp\{-4\delta^2/\Delta t\}}{\Delta t}\right)$$

for $\vec{z}$, $\vec{x}$ on Γ, where it is assumed that Γ is always at a distance equal to or greater than δ from the boundary of the box. Thus, as a first approximation, for small Δt, the single layer potential in equation (19) can be given by:

$$\begin{aligned}&\int_0^{\Delta t}\int_\Gamma G(\vec{z}, \vec{x}, \Delta t, \tau) q(\vec{x}, \tau + (t_l - \Delta t)) d\Gamma_{\vec{x}} d\tau \\ &= \int_0^{\Delta t}\int_\Gamma u^*(\vec{z}, \vec{x}, \Delta t, \tau) q(\vec{x}, \tau + (t_l - \Delta t)) d\Gamma_{\vec{x}} d\tau + O\left(\exp\{-4\delta^2/\Delta t\}\right)\end{aligned} \tag{20}$$

Similarly, $\frac{\partial G(\vec{z}, \vec{x}, \Delta t, \tau)}{\partial n_{\vec{x}}}$ can approximate to

$$q^*(\vec{z}, \vec{x}, \Delta t, \tau) = \frac{\partial u^*(\vec{z}, \vec{x}, \Delta t, \tau)}{\partial n_{\vec{x}}} = \frac{d}{8\pi\alpha^2(\Delta t - \tau)^2} \exp\left(-\frac{\| \vec{z} - \vec{x} \|^2}{4\alpha(\Delta t - \tau)}\right)$$

as $\Delta t \to 0$ with $d = [z_1 - x_1] \cdot n_{\vec{x}_1} + [z_2 - x_2] \cdot n_{\vec{x}_2}$.

In fact, q^* is the leading term of the series

$$\frac{\partial G(\vec{z},\vec{x},\Delta t,\tau)}{\partial n_{\vec{x}}} = \frac{1}{8\pi\alpha^2(\Delta t-\tau)^2}\cdot$$
$$\cdot\sum_{m\in Z^2}\sum_{\sigma_i=\pm 1}\left[-\sigma_1^2\sigma_2(z_1-\sigma_1x_1-2m_1L_x)n_{1_x}-\sigma_1\sigma_2^2(z_2-\sigma_2x_2-2m_2L_y)n_{2_x}\right] \quad (21)$$
$$\cdot\exp\left\{-\parallel\vec{z}-\sigma\vec{x}-2\vec{m}L\parallel^2/4\alpha(\Delta t-\tau)\right\}$$

which corresponds to $\vec{m}=\vec{0}$, $\sigma_i=1$, $i=1,2$. Then,

$$\left|\frac{\partial G(\vec{z},\vec{x},\Delta t,\tau)}{\partial n_{\vec{x}}}-q^*(\vec{z},\vec{x},\Delta t,\tau)\right| = O\left(\frac{2\delta}{(\Delta t)^2}\exp\left\{-4\delta^2/\Delta t\right\}\right)$$

for $\vec{z}$, $\vec{x}$ on Γ. Thus, the double layer potential for small Δt can be approximated by:

$$\begin{aligned}\int_0^{\Delta t}\int_\Gamma \frac{\partial G(\vec{z},\vec{x},\Delta t,\tau)}{\partial n_{\vec{x}}}u(\vec{x},\tau+(t_l-\Delta t))d\Gamma_{\vec{x}}d\tau \\ = \int_0^{\Delta t}\int_\Gamma q^*(\vec{z},\vec{x},\Delta t,\tau)u(\vec{x},\tau+(t_l-\Delta t))d\Gamma_{\vec{x}}d\tau \\ + O\left(\frac{2\delta}{\Delta t}\exp\left\{-4\delta^2/\Delta t\right\}\right)\end{aligned} \quad (22)$$

as $\Delta t\to 0$.

On the other hand, the truncation error of the double series in equation (19) can be proved to be $O(\frac{e^{-p^2}}{p})$ (for more details see Appendix 1), where p is the number of terms used in the numerical evaluation of the series, and therefore only a small number of terms need to be considered in the evaluation of the series due to its exponential convergence.

After considering the above error estimations for the approximation of the single layer, double layer and the double series in equation (19), and discretizing the surface Γ in order to carry out all the contour integrals involved in the evaluation of equation (19), we finally arrive at the following BEM approximation for small values of Δt of our integral equation:

$$\begin{aligned}c_iu_f^i+\alpha\sum_{j=1}^{N}\left(\int_0^{\Delta t}\int_{\Gamma_j}\varphi^T\psi q^*d\Gamma dt\right)u^n = \alpha\sum_{j=1}^{N}\left(\int_0^{\Delta t}\int_{\Gamma_j}\varphi^T\psi u^*d\Gamma dt\right)q^n \\ +\frac{4}{L_xL_y}\sum_{k_1=1}^{p}\sum_{k_2=1}^{p}\exp\left(-\pi^2k^2\alpha\Delta t\right)I_{k_1k_2}(t_{f-1})\sin\pi\frac{k_1}{L_x}\xi_1^i\sin\pi\frac{k_2}{L_y}\xi_2^i\end{aligned} \quad (23)$$

In the above equation the functions φ and ψ are the space and time interpolation functions, respectively.

Using the estimation of the truncation error of the double series given in Appendix 1, which is a function of the value of Δt, position of the domain in the box, size of the box and the number of terms in the series, we can choose the number of terms in the series for a given problem, value of Δt and desired accuracy.

In the BEM solution of the above equation, the contour Γ was discretized using straight-line elements, in which the functions u and q were assumed to vary linearly within each element in space and time. The evaluation of the above single and double layer potentials at the regular elements, i.e. when the collocation point is not at the integration element, was carried out numerically using Gauss quadrature. On the other hand, at the singular elements, i.e. when the collocation point lies on the integration element, the space integration of the single layer potential was evaluated analytically (see Appendix 3) and the time integration, numerically, using Gauss quadrature. In our case (linear elements), the integration is not necessary at the singular element of the double layer potential owing to the orthogonality between $\vec{r}$ ($\vec{r} = \vec{z} - \vec{x}$) and $\vec{n}$, which makes zero the value of the normal derivative of $\vec{r}$.

In order to improve the accuracy of the integration scheme, Telles's (1987) transformation was always used in the numerical evaluation of the time integration. The resulting algebraic system for the unknown surface temperature or flux was solved using a standard Gauss procedure.

It is important to observe that all the integrals in equation (23), which are only of the contour type, need to be evaluated only once, at the beginning of the time stepping process. In particular, the moment integrals of each boundary element, which are required to evaluate the Fourier coefficients in the double series representation of the domain integral, are only a function of the number of terms used in the double series.

In the general case of non-zero initial condition, it is possible to use the recursion formula, equation (16), with the initial term $I_{k_1 k_2}(0)$ given by the domain trigonometric moments of the initial temperature field, i.e.

$$I_{k_1 k_2}(0) = \int_{\Omega} u(\vec{x}, 0) \sin \frac{\pi k_1 x_1}{L_x} \sin \frac{\pi k_2 x_2}{L_y} d\Omega$$

If the initial condition corresponds to the solution of the steady state heat equation, i.e. a harmonic function, it is possible to transform exactly the initial domain integral into surface integrals (see Brebbia *et al.*, 1984).

In section 5 of this paper, we will analyse the improvement obtained in the present approach when more terms than the free space fundamental solution are used in the approximation of the Green function on the kernels of the above single and double layer potentials, which are required in order to be able to increase the value of Δt used in the numerical algorithm. The corresponding truncation error in the approximation of the single and double layers can be obtaining by adding to equations (20) and (22) the extra terms of the series.

4. Numerical results

(i) Accuracy comparison

In order to test the efficiency and the accuracy of the proposed numerical scheme, several examples with different boundary conditions were solved for the same region, i.e. a 0.5×0.5 square region located in the centre of $B = [0, 1] \times [0, 1]$, with initial temperature $u_0 = 0$ and thermal diffusivity $\alpha = 1$. For all of them, no flow of heat will be prescribed at the sides $y = 0.25$ and $y = 0.75$; this non-flux condition reduces the problem to the one-dimensional one, for which analytical solutions are available.

Example 1. Constant flux equal to 1 on the wall $x = 0.75$, and equal to –1 on $x = 0.25$. It is well-known that in this example the temperature reaches the steady state given by the expression $u(x) = (x - 0.5)$. In our numerical result, the steady state condition was achieved at the time $t = 0.39$; similar value of such time was obtained when the standard convolution scheme was employed (denoted by Brebbia *et al.* (1984) as scheme 2).

In Figure 3 we present the comparison between our numerical solution for different times and those obtained with the convolution time stepping scheme (scheme 2), showing excellent agreement.

Some tests were carried out to study how the number of terms in the series affects the solution. In Table I, we compare the steady state numerical solution obtained with the present approach using a different number of terms in the series, with those obtained with scheme 2 and the analytical solution. From this comparison, it is possible to observe that the series to evaluate the domain integral converges quite fast and hence an accurate solution can be obtained with only a few terms of the series. A maximum difference of 0.04 per cent

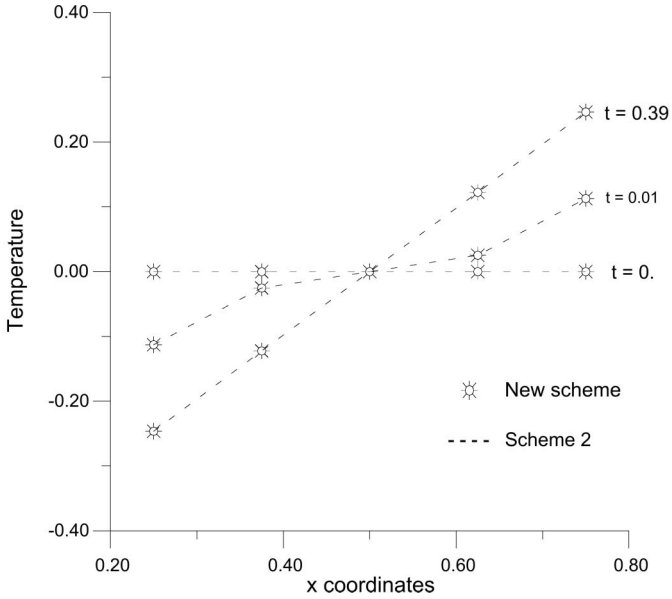

Figure 3.
Transient temperature profiles

x	y	$k = 5$	$k = 10$	$k = 20$	Scheme 2	Analytical solution
0.25	0.25	–0.2493857	–0.2498485	–0.2498485	–0.2499575	–0.25
0.375	0.25	–0.1251118	–0.1249383	–0.1249382	–0.1249712	–0.125
0.5	0.25	–0.1274E-7	–0.1233E-7	–0.1233E-7	–0.6466E-8	0
0.625	0.25	0.1251117	0.1249382	0.1249382	0.1249711	0.125
0.75	0.25	0.2493857	0.2498486	0.2498485	0.2499575	0.25
0.75	0.25	0.2493857	0.2498486	0.2498485	0.2499575	0.25
0.75	0.375	0.2492108	0.2498966	0.2498966	0.2499767	0.25
0.75	0.5	0.2494113	0.2498959	0.2498960	0.2499767	0.25
0.75	0.625	0.2492108	0.2498966	0.2498966	0.2499767	0.25
0.75	0.75	0.2493857	0.2498486	0.2498485	0.2499575	0.25
0.75	0.75	0.2493857	0.2498486	0.2498485	0.2499575	0.25
0.625	0.75	0.1251117	0.1249382	0.1249382	0.1249711	0.125
0.5	0.75	–0.1089E-7	–0.1048E-7	–0.1048E-7	–0.5739E-8	0
0.375	0.75	–0.1251118	–0.1249383	–0.1249382	–0.1249712	–0.125
0.25	0.75	–0.2493857	–0.2498486	–0.2498485	–0.2499575	–0.25
0.25	0.75	–0.2493857	–0.2498486	–0.2498485	–0.2499575	–0.25
0.25	0.625	–0.2492108	–0.2498967	–0.2498966	–0.2499767	–0.25
0.25	0.5	–0.2494113	–0.2498960	–0.2498960	–0.2499768	–0.25
0.25	0.375	–0.2492108	–0.2498967	–0.2498966	–0.2499767	–0.25
0.25	0.25	–0.2493857	–0.2498486	–0.2498485	–0.2499575	–0.25

Table I. Surface temperature at time $t = 0.39$

between the two numerical schemes was found when only ten terms were used in the evaluation of the trigonometric series. The evaluation of such series can be improved and computed more efficiently if we make use of Rokhlin's non-equidistant fast Fourier transform algorithm, which makes the interpolation error decay superalgebraically (for more details see Strain, 1992). The time step used in the above analysis was 0.01 and the BEM discretization employed 16 linear elements and 20 nodes (there are four double nodes at the intersections of the boundary walls, i.e. the corners).

Example 2. Constant flux equal to 5 at $x = 0.75$ and no flow of heat over the remaining boundary.

The analytical solution of internal temperature distribution consists of a term that increases linearly with time, plus a correcting term which depends on the position and the time. It is of the form:

$$u(x,t) = 10t + 10\left[\frac{3(x-0.25)^2 - 0.25}{6}\right] - \frac{20}{\pi^2}\sum_{n=1}^{\infty}\frac{(-1)^n}{n^2}e^{-n^2\pi^2 t/0.25}\cos\frac{n\pi(x-0.25)}{0.5}$$

The evolution solutions presented in Figure 4 correspond to the one obtained with scheme 2 and the new scheme, showing an excellent match between them.

As before, both numerical schemes agree perfectly with the above analytical solution.

In the numerical solution of this example, for both schemes, we used 32 nodes on the boundary (four are double) and a time step of 0.01.

Example 3. The flux is given as a prescribed function of the time equal to $5t$ over $x = 0.75$ and no flow of heat over the remaining boundary.

Table II shows the results obtained with the new scheme with $k = 10$ and $k = 50$ terms, after 100 time steps of size 0.01. Both results were compared with those obtained with scheme 2. As can be seen, the agreement is really excellent. The two schemes used linear variations for u and q, where 16 elements and a time step of 0.01 were utilized.

The variation of the surface temperature with time is presented in Figure 5. From which can be observed the good match between the solutions using the two schemes.

Example 4. Mixed boundary conditions: constant flux equal to 1 on the wall at $x = 0.75$, and the wall at $x = 0.25$ is kept at zero temperature.

The analytical solution is given by

$$u(x,t) = (x - 0.25) - \frac{4}{\pi^2}\sum_{n=0}^{\infty}\frac{(-1)^n}{(2n+1)^2}e^{-(2n+1)^2\pi^2 t}\sin[(2n+1)\pi(x-0.25)]$$

for $0.25 \leq x \leq 0.75$, $t \geqslant 0$.

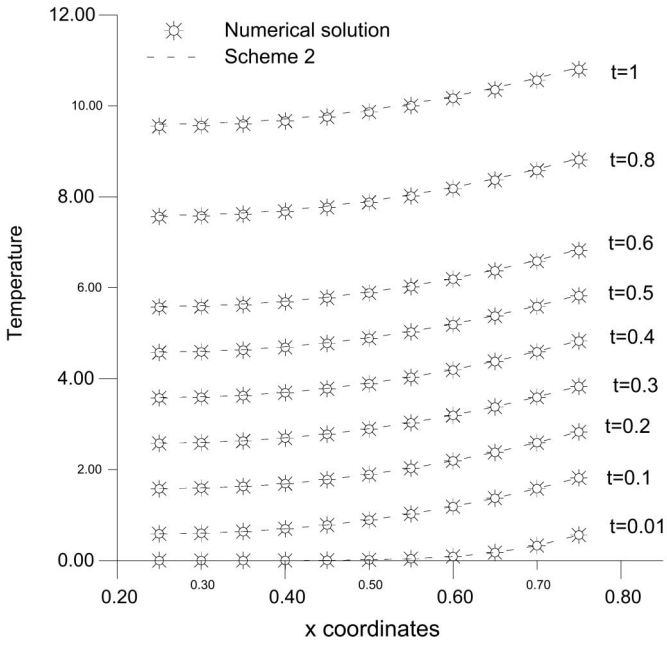

Figure 4.
Transient temperature profiles on the boundary

x	y	$k = 10$	$k = 50$	Scheme 2
0.25	0.25	4.634175	4.634146	4.624805
0.375	0.25	4.710933	4.710905	4.701217
0.5	0.25	4.936919	4.936895	4.927359
0.625	0.25	5.317900	5.317872	5.308205
0.75	0.25	5.857710	5.857681	5.848511
0.75	0.25	5.857710	5.857681	5.848511
0.75	0.375	5.863567	5.863539	5.854755
0.75	0.5	5.862673	5.862650	5.854403
0.75	0.625	5.863567	5.863539	5.854755
0.75	0.75	5.857710	5.857681	5.848511
0.75	0.75	5.857710	5.857681	5.848511
0.625	0.75	5.317900	5.317872	5.308205
0.5	0.75	4.936919	4.936895	4.927359
0.375	0.75	4.710932	4.710905	4.701217
0.25	0.75	4.634174	4.634145	4.624805
0.25	0.75	4.634174	4.634145	4.624805
0.25	0.625	4.639486	4.639458	4.630592
0.25	0.5	4.638707	4.638683	4.630322
0.25	0.375	4.639486	4.639459	4.630592
0.25	0.25	4.634175	4.634146	4.624805

Table II.
Results on the boundary for $T = 1$

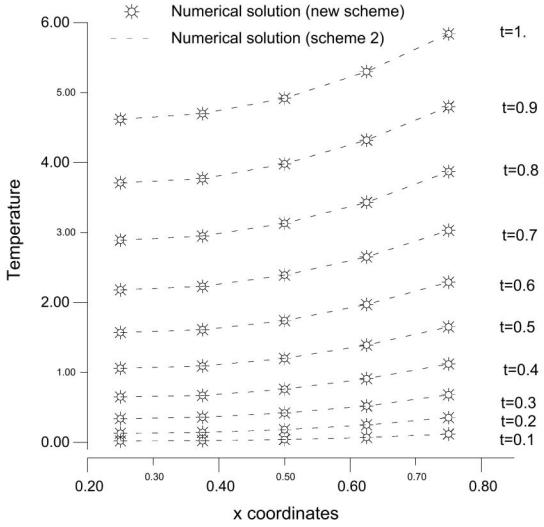

Figure 5.
Transient temperature profiles

Figure 6 shows a graphic comparison between the numerical solution and analytical solution, where it is possible to observe the close match between them. In the analysis of the numerical results, it was considered that the steady state was reached when the norm of the difference between the temperatures on each point of the surface at time t and $t - \Delta t$ was lower than 10^{-4}. In fact, the

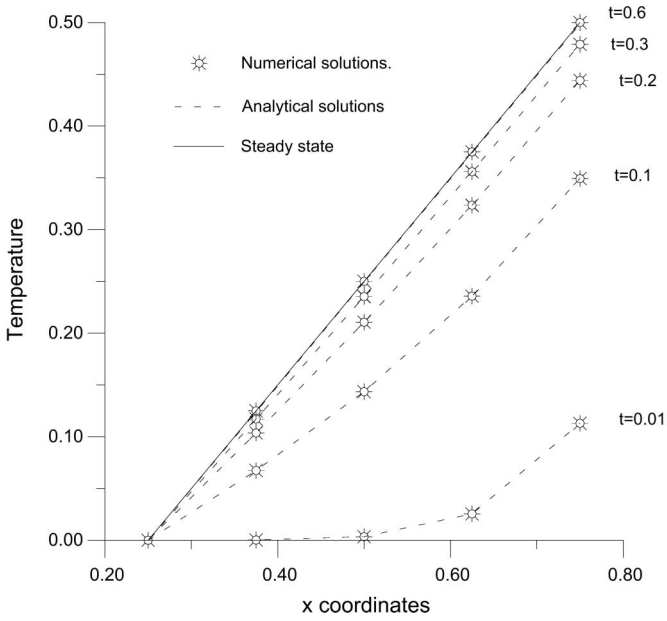

Figure 6.
Transient temperature profiles

numerical steady state was achieved at $t = 0.64$, where Δt was prescribed equal to 0.01 and the solutions were obtained using only five terms in the Fourier series.

The relative error between the exact steady state solution and its approximation is no bigger than 1 per cent; so it shows the accuracy of the new scheme for few terms in the series.

(ii) CPU-time comparison

To compute the algorithmic complexity of a convolution scheme of the heat integral equation, it is necessary to consider the task of calculating the potentials at a sequence of time levels $t = \Delta t, 2\Delta t, \ldots, (M-1)\,\Delta t$. Therefore, at the $M - th$ level, it must be summed over all previous levels, resulting in the following total work: $2N^2$ operations to obtain each of the potentials at each time step, and at the last time step it is required to build the matrix system and solve it, i.e. N^2 and N^3 operations, respectively. In this way $(N^2 + N^3 + 2N^2 (M-1))\,M$ operations are computed to solve the heat equation up to a fixed time $T = M\Delta t$, which is the dominant order for a large time T, i.e. $M \gg N$, gives $O(N^2 M^2)$.

As was mentioned before, the basic idea of the new scheme is to use the time dependant fundamental solution in the integral representation and to approximate the evolution of the domain integral using Fourier series. The time integration is performed only over one time step and the history is transformed in a domain integral, which can be approximated using Fourier series, which coefficients at every time step are computed from those of the previous step. Therefore, the new scheme requires a computational cost of $N^2 + (N^2 + N^3 +$

N^2p^2) M, where the direct evaluation of the series would require $O(N^2p^2)$, where p is the number of terms in each series, which is in general very small, $p \ll N$. Therefore, for a large time T, the dominant order of the computational cost is O (N^3M), with $M \gg N$. This results in huge savings in terms of CPU-time compared with the CPU-time required by the convolution approach. If the re-initialization scheme with direct evaluation of the domain integral is used, $LN^2 + (N^2 + N^3 + LN^2)\ M$ operations are required to obtain the solution at time T, where L is the number of internal points used to evaluate the domain integral, which in general is very large $L \gg N$. For a large time this approach results in a complexity of the order O (LN^2M). It can be observed from the previous analysis that the order in both reinitialization schemes is linear but the slope corresponding to the new scheme is smaller resulting in smaller CPU-time for the mentioned algorithm.

To demonstrate this fact, we consider the problem of a circular region of radius 0.1 and centre (0.5, 0.5) contained in the box $B = [0, 1] \times [0, 1]$. The initial condition was taken as equal to zero and as boundary condition the flux was prescribed equal to 3 and the thermal diffusivity equal to 1.

The problem was solved using scheme 2 and the new scheme with the same computational platform. Figure 7 shows that the CPU-time for the new scheme increases slightly and linearly with the number of time steps and the CPU-time for scheme 2 behaves like a curve of order two. So, when computations are to be performed for a large number of time steps, the new scheme represents a huge saving in CPU-time.

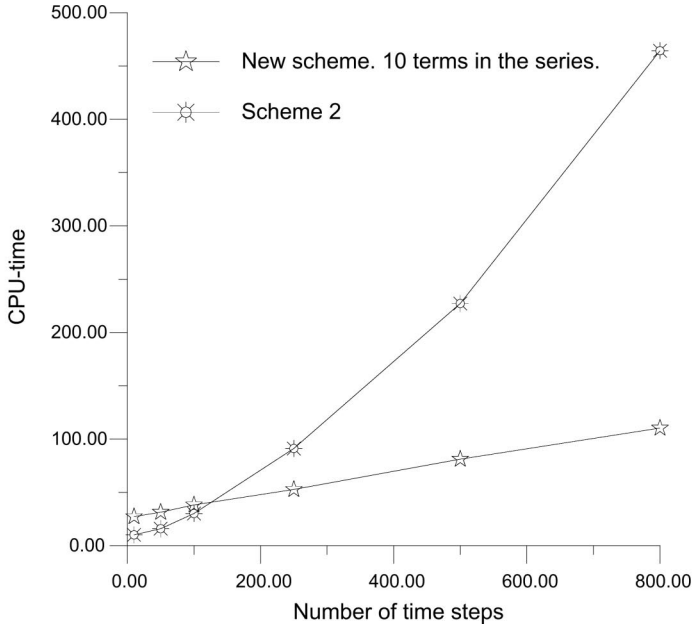

Figure 7.
Comparison of accumulated CPU-time in seconds for the new scheme (re-initialization scheme) and scheme 2 (convolution scheme), using $\Delta t = 0.01$

The solutions obtained using the two schemes were in excellent agreement with the analytical solution. In fact, the relative error of the surface temperature calculated with the new scheme, at number of time steps of 10, 50, 100, 250, 500, 800, was never bigger than 0.5 per cent, as is shown in Table III.

5. Refined approach by adding images

As noted previously, the convergence rate of the scheme is mainly dependent on the order of the local approximation of the kernels in the single and double layer potential.

In several tests, the results show that the scheme is very sensitive to changes in the magnitude of δ and Δt, i.e. to the value of the minimum distance from the boundary Γ to the boundary of the box B and the size of the time step. The error was bigger when $\delta \to 0$ and when Δt increases because the term $e^{-4\delta^2/\Delta t}$, in equations (20) and (22), tends to one.

In order to handle these two situations, we approximated the Green function G by the free-space kernel plus the closer images to the box's contour, in such a manner that the above term reduces to $e^{-((2+r)\delta)^2/\Delta t}$, where $(2 + r)\delta$ is the minimum distance from the boundary to the further image, i.e.

$$G(\vec{z},\vec{x},T,t) \tilde{=} \frac{1}{4\pi\alpha(T-t)} \sum_{\substack{m_1=-r \\ m_2=-r}}^{r} \sum_{\sigma_i=\pm 1} \sigma_1\sigma_2 \exp\left\{ -\frac{\|\vec{z} - \sigma\cdot\vec{x} - 2\vec{m}L\|^2}{4\alpha(T-t)} \right\}$$

and analogously

$$\frac{\partial G(\vec{z},\vec{x},T,t)}{\partial n_{\vec{x}}} \tilde{=} \frac{1}{8\pi\alpha^2(T-t)^2} \cdot \sum_{\substack{m_1=-r \\ m_1=-r}}^{r} \left[\sum_{\sigma_{1,2}=\pm 1} -\sigma_1^2\sigma_2(z_1 - \sigma_1 x_1 - 2m_1 L_x) n_{1_x} \right.$$

Number of time steps	New scheme CPU-time temperature	Scheme 2 CPU-time temperature	Analytical solution temperature
10	27.332	10.1718	
	6.09823	6.1009	6.075
50	31.4218	15.9414	
	30.2298	30.2524	30.075
100	38.3085	30.25	
	60.3576	60.42527	60.075
250	52.800	91.1875	
	150.4977	150.9798	150.075
500	81.1992	227.1992	
	299.9236	301.8931	300.075
800	110.3398	464.3594	
	477.9107	483.0059	480.075

Table III.
Results for the CPU-time and temperature at different number of time steps

$$-\sigma_1\sigma_2^2(z_2-\sigma_2 x_2-2m_2L_y)n_{2_x}]\cdot\exp\left\{\frac{-\parallel\vec{z}-\sigma\vec{x}-2\vec{m}L\parallel^2}{4\alpha(T-t)}\right\}$$

Example 5. As an example of the application of the above technique, consider the problem of determining the temperature on the boundary surface of a circular region Γ contained in the box $B = [0, 1] \times [0, 1]$, with centre $(0.5, 0.5)$, subjected to the boundary flux condition $q = 3$ along Γ for any time $t > 0$, zero initial temperature and thermal diffusivity $\alpha = 1$.

The analytical solution for this problem is given by the expression:

$$u(\rho,t)=\frac{2qt}{a}+qa\left\{\frac{\rho^2}{2a^2}-\frac{1}{4}-2\sum_{n=1}^{\infty}e^{-\frac{\pi\beta_n^2 t}{a^2}}\frac{J_0\left(\frac{\rho\beta_n}{a}\right)}{\beta_n^2 J_0(\beta_n)}\right\}$$

where β_n, $n = 1, 2, \ldots$, are the positive roots of $J_1(\beta) = 0$ and a is the radius of the circle Γ

Figure 8 shows the relative error of the surface temperature obtained in the case of a circle of radius 0.25 for different sizes of the time step and different terms in the image system. It can be observed that the numerical solution is improved adding images to the kernel on the surface integrals. Up to a time step of 0.01 the solution without images is in very good agreement with the analytical one. For time steps greater than 0.01, several images of the source

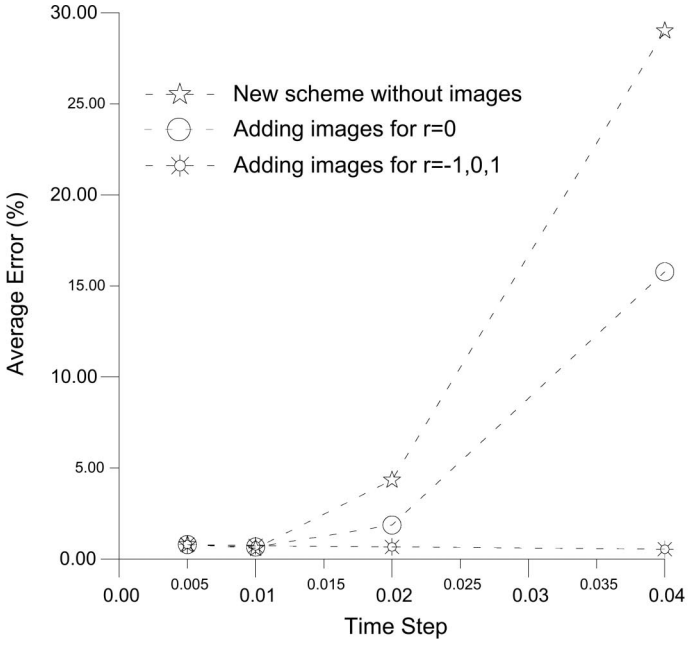

Figure 8.
Relative error in the numerical solution at final time $T = 1$, for different time steps

points were added, in order to obtain a good accuracy. When using the image corresponding to the series $-1 \leq r \leq 1$, the accuracy obtained was independent of the size of the time step tested, $0.005 \leq \Delta t \leq 0.04$.

In order to consider the relation between δ, the distance from the surface Γ to the box boundary B, and the precision of the numerical results when the image system is included, the above example was repeated for different sizes of the circular region and a fixed time step, in Figure 9 we present some values of the relative error in the numerical solution of the surface temperature at the final time $T = 1$, for the case of three circular regions centred at (0.5, 0.5) with radii $a = 0.1, 0.25, 0.4$. The choice of the time step was 0.02. From this Figure, it can be appreciated that when δ decreases the solution can be improved by adding more images to the fundamental solution. Again, when the images corresponding to the series $-1 \leq r \leq 1$ were added, the accuracy obtained was independent of the size of the distance δ tested, $0.1 \leq \delta \leq 0.4$.

An alternative, for using bigger time steps without adding images, is to look for the numerical solution using different size of the square box. In this way the error in the local approximation is lower if the distance from the boundary to the box is bigger but more terms in the series representation of the domain integral will be necessary. To demonstrate that situation, we analysed the case of a circle with radius 0.1 and located in the centre of the box. The solution was found at time $T = 1$ to compare with the analytical value of 60.075.

In order to chose the appropriate number of terms in the Fourier series, to reach a reasonable numerical accuracy, without unnecessary calculations, it was required that

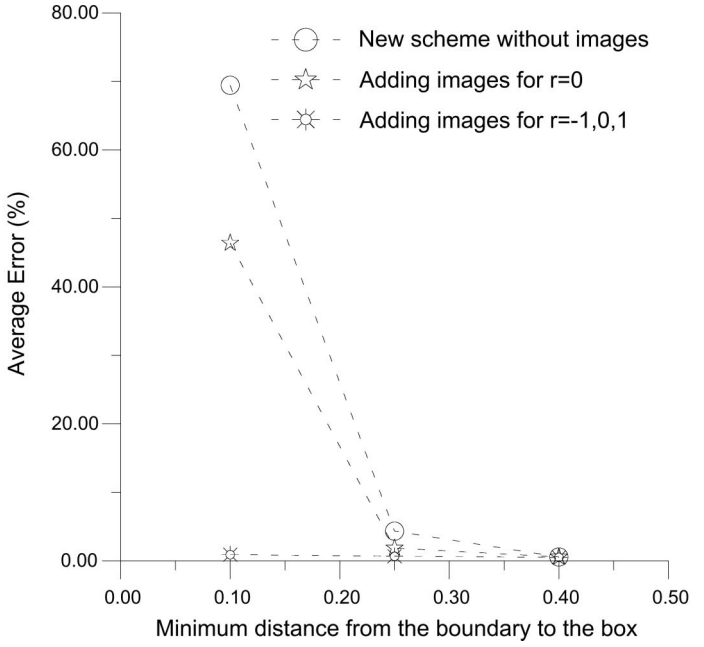

Figure 9.
Average errors vs. distance from Γ to B, using a time step of 0.02

$$\exp\left(-\pi^2 k^2 \alpha \Delta t\right) \geq 10^{-6}$$

or making some manipulations, $\frac{p^2 \alpha \Delta t}{L^2} \leq 0.7$, where L is the minimum value between L_x and L_y, p maximum number of terms in the truncated series and Δt size of time step.

In Table IV are shown the numerical solutions for different size boxes B_0 = [0, 1] × [0, 1], B_1 = [0, 5] × [0, 5], B_2 = [0, 10] × [0, 10], using only the fundamental solution in the approximation of the Green function. It can be observed that with the boxes B_1 and B_2 it was possible to obtain an accurate solution with an error lower than 0.5 per cent with a value of $\Delta t = 0.05$; this precision was obtained with the box B_0 when the value of Δt was 0.02. An error of 2 per cent was obtained with the boxes B_1 and B_2 when the value of Δt was 0.1. It is also interesting to observe from Table IV that fewer terms on the series expansion are required when the value of Δt increases, but the accuracy of the solution reduces.

6. Other related schemes

As mentioned in the introduction, the works by Davey and Bounds (1996) and Zerroukat (1998) present several similarities to and differences from the present work that are worthy of special attention. All of these schemes are of the re-initialization type, in which the corresponding domain integrals are transformed into a truncated series representation, which coefficients can be determined in terms of a recursive formula from previous time step. Besides, the three schemes have the same computational complexity of $O(M)$ in time.

In Zerroukat's (1998) work, the terms of the truncated series are given by cell integrations over the problem domain of the product of the heat fundamental solution and some radial basis functions. The coefficients of the series are obtained by means of a radial basis function collocation method developed by Kansa (1990), which is used to find particular solutions of the heat equation in terms of known values of the temperature field at the previous time step. The main computational problem of this approach lies in the evaluation of the internal temperature field, which requires that at each surface element the single and the double layer potentials in equation (5) need to be evaluated a number of times equal to the number of surface collocations points plus the internal points. Although intensive research activity is going on in the topic of radial basis function collocation method, no formal mathematical proof of the

Δt	$B_0 = [0,1] \times [0,1]$	$B_1 = [0,5] \times [0,5]$	$B_2 = [0,10] \times [0,10]$
0.01	u = 60.454, p = 5	u = 60.384, p = 41	u = 60.380, p = 83
0.02	u = 60.3917, p = 5	u = 60.5794, p = 29	u = 60.5784, p = 59
0.04	u = 57.8033, p = 5	u = 59.946, p = 26	u = 59.9486, p = 52
0.05	u = 54.6123, p = 5	u = 60.3656, p = 18	u = 60.3619, p = 36
0.1	u = 40.98, p = 5	u = 61.4216, p = 13	u = 61.4042, p = 26

Table IV. Temperature u at time T = 1, using p terms in the series defined on the box B_i, i = 0, 1, 2

solvability and convergence of Kansa (1990) method is available in the literature. This lack of mathematical formality suggests the use of this approach with caution.

On the other hand, in Davey and Bounds' (1996) work the terms of the truncated series are given by single and double layer surface potentials obtained by representing the heat fundamental solution in the domain integral of equation (5) in terms of a linear superposition of finite number of heat sources positioned at different points in time. The coefficients of such representation of the fundamental solution are obtained by a minimization of the interpolation error by using a single point exchange algorithm, which requires an iterative procedure. As in Zerroukat's (1998) work, in this approach at every surface element, each of the single and double layer surface potentials corresponding to each of the heat sources positioned at different points in time needs to be evaluated a number of times equal to the number of surface collocation points.

Despite the fact that it is possible to guarantee that the time truncated series representation of the fundamental solution given by Davey and Bounds (1996) and the present space series representation can be improved by including additional source terms in the corresponding series, only in the present approach is it possible to have an error indicator of such truncation given in terms of the remainder of the double Fourier series, which can be used to estimate the concurrent error in the corresponding surface integrals.

In contrast with these two works, in the present approach, the terms of the series are trigonometric sine and cosine functions, and the resulting coefficients are given in terms of the surface integrals of some trigonometric moments of the surface elements, which are independent of the number of collocation points and the evaluation time. This is due to the uncoupled behaviour of the independent variables of the single and double layer potential kernels when the Green function is approximated by a function of the degenerate type, i.e. the truncated form of equation (7). A major consequence of this type of degenerate function is that it is possible to introduce new surface elements in the algorithm to evaluate the domain integrals without requiring to perform revaluation of the integrals on the previous elements, as will be the case with the two other approaches. This is an important feature when dealing with mesh refinement scheme or solving moving boundary problems. Also, in the present case we can change the time step of algorithm without any major modification; it is only required to multiply the Fourier coefficients by a constant value. This is not the case when this change is performed with any of the two other approaches, which require the revaluation of all the integrals involved in the series representation of the domain integral. In the three methods, the single and double layer potentials at the time interval $t_l - \Delta t$ and t_l need to be revaluated when the time step is changed.

For simple problems such as the one presented in this work, these three $O(M)$ schemes have similar computational cost. However, it is expected that for

complex problems that involve mesh refinement, change in time step and moving boundary, the approach proposed in this work will be simpler in implementation and less costly than the other two.

7. Conclusions

The numerical results shown clearly demonstrate that the new scheme achieves similar results to those of the classical direct boundary element method but with huge savings in the computational cost. Unlike the direct method, the new scheme removes the history dependence and allows the solution at any time step to be calculated with a relatively constant CPU-time.

It is important to point out that Greengard and Strain (1990), and subsequently Sethian and Strain (1992) and Strain (1992), solved several heat transfer problems with Dirichlet boundary conditions, in bounded domains, using the Fourier representation of the Green function in an indirect BEM formulation given in terms of a single layer potential alone, which represents a regular continuous temperature field inside the entire box B. On the other hand, the use of such Green function on the Green integral representation formula yields to an expression equal to temperature field inside Ω, and zero value in the exterior domain to Ω, bounded by ∂B and Γ, with a limiting value at a point $\vec{\xi}$ on the boundary Γ equal to $c\left(\vec{\xi}\right)\ u\ \left(\vec{\xi}, T\right)$. This discontinuous behaviour allowed us to evaluate the domain integrals in a resourceful manner, knowing only the temperature and flux boundary values at the previous time step, without the explicit values of the internal temperature. The consecutive evaluation of such domain integrals was obtained in terms of a regular double Fourier series for a discontinuous function inside the box, which it is not possible to use when the Greengard and Strain (1990) indirect approach is utilized due to the continuity property of the single layer potential across its density carrying surface.

The present direct formulation enables us to solve different types of the boundary values problem without changing the integral equation formulation of the problem, which it is not possible to achieve if an indirect formulation is employed instead of the present direct formulation.

References

Brebbia, C.A., Telles, J.C.F. and Wrobel, L.C. (1984), *Boundary Element Techniques. Theory and Applications in Engineering*, Springer-Verlag, Berlin.

Carslaw, H.S. and Jaeger, J.C. (1959), *Conduction of Heat in Solids*, 2nd ed., Clarendon Press, Oxford.

Chang, Y.P., Kang, C.S. and Chen, D.J. (1973), "The use of fundamental Green's functions for the solution of problems of heat conduction in anisotropic media", *Int. J. Heat Mass Transf.*, Vol. 16, pp. 1905-18.

Davey, K. and Bounds, S. (1996), "Source-weighted domain integral approximation for linear transient heat conduction", *Int. J. Numer. Meths Eng.*, Vol. 39, pp. 1775-90.

Davey, K. and Hinduja, S. (1987), "An improved procedure for solving transient heat conduction problems using the boundary element method", *Int. J. Numer. Meths Eng.*, Vol. 28, pp. 2293-306.

Demirel, V. and Wang, S. (1987), "An efficient boundary element method for two-dimensional transient wave propagation problems", *Appl. Maths Modelling*, Vol. 11, pp. 411-16.

Dym, H. and McKean, H.P. (1972), *Fourier Series and Integrals*, Academic Press, New York and London.

Greengard, L. and Strain, J. (1990), "A fast algorithm for the evaluation of heat potentials", *Communications on Pure and Applied Mathematics*, Vol. XLIII, John Wiley & Sons, pp. 949-63.

Hsiao, G.C. and Saranen, J. (1993), "Boundary integral solution of the two-dimensional heat equation", *Mathematical Methods in the Applied Sciences*, Vol. 16, pp. 87-114.

Kansa, E.J. (1990), "Multiquadrics – a scattered data approximation scheme with applications to computation fluid dynamics II: solution to parabolic, hyperbolic and elliptic partial differential equations", *Computers Math. Applic.*, Vol. 19, pp. 147-61.

Knopp, K. (1956), *Infinite Sequences and Series*, Dover, New York, NY.

Mikhlin, S.G. (1957), *Integral Equations and their Applications to Certain Problems in Mechanics, Mathematical Physics and Technology*, Pergamon Press.

Morse, P.M. and Feshbach, H. (1953), *Methods of Theoretical Physics*, McGraw-Hill, New York, NY.

Sethian, J.A. and Strain, J. (1992), "Crystal growth and dendritic solidification", *Journal of Computational Physics*, Vol. 98, Academic Press, Inc., pp. 231-53.

Shaw, R.P. (1974), "An integral equation approach to diffusion", *Int. J. Heat Mass Transf.*, Vol. 17, pp. 693-9.

Singh, K.M. and Kalra, M.S. (1995), "Application of cubic Hermitian algorithms to boundary element analysis of heat conduction", *Int. J. Numer. Meth. Eng.*, Vol. 38, pp. 2639-51.

Strain, J. (1992), "Fast potential theory. II. Layer potentials and discrete sums", *Journal of Computational Physics*, Vol. 99, Academic Press, Inc., pp. 251-70.

Telles, J.C.F. (1987), "A self-adaptive co-ordinate transformation for efficient numerical evaluation of general boundary element integrals", *Int. J. Num. Meths Eng.*, Vol. 24, pp. 959-73.

Tolstov, G.P. (1962), *Fourier Series*, Dover Publications, Inc., New York, NY.

Wrobel, L.C. and Brebbia, C.A. (1979), "The boundary element method for steady-state and transient heat conduction", in Lewis, R.W. and Morgan, K. (Eds), *Numerical Methods in Thermal Problems*, Vol. 1, Pineridge Press, Swansea.

Zerroukat, M. (1998), "A fast boundary element algorithm for time-dependant potential problems", *Applied Mathematical Modelling*, Vol. 22, pp. 183-96.

Zerroukat, M. and Power, H. (1998), "On time-dependent domain integral approximation using radial basis functions", *Boundary Elements XX, Advances in Boundary Elements*, Computational Mechanics Publications.

Zerroukat, M., Power, H. and Chen, C.S. (1998), "A numerical method for heat transfer problems using collocation and radial basis functions", *Int. J. Numer. Meth. Engng*, Vol. 42, pp. 1263-78.

Appendix 1

Let us estimate the magnitude of the truncation error (E_p) of the double series in equation (19) after using k_i terms, with $k_i = p$, $i = 1, 2$. For simplicity we will consider a square box B, i.e. $L_x = L_y$.

$$| E_p | = \frac{4}{L_x L_y} | \sum_{k_1=1}^{p} \sum_{k_2=p+1}^{\infty} \exp\left(-\pi^2 k^2 \alpha \Delta t\right) I_{k_1 k_2}\left(t_{f-1}\right) \sin \pi \frac{k_1}{L_x} \xi_1 \sin \pi \frac{k_2}{L_y} \xi_2 +$$

$$\sum_{k_1=p+1}^{\infty}\sum_{k_2=1}^{\infty}\exp\left(-\pi^2k^2\alpha\Delta t\right)I_{k_1k_2}\left(t_{f-1}\right)\sin\pi\frac{k_1}{L_x}\xi_1\sin\pi\frac{k_2}{L_y}\xi_2\mid$$

$$\leq\frac{4}{L_xL_y}\sum_{k_1=1}^{\infty}\sum_{k_2=p+1}^{\infty}\mid\exp\left(-\pi^2k^2\alpha\Delta t\right)I_{k_1k_2}\left(t_{f-1}\right)\sin\pi\frac{k_1}{L_x}\xi_1\sin\pi\frac{k_2}{L_y}\xi_2\mid$$

$$+\frac{4}{L_xL_y}\sum_{k_1=p+1}^{\infty}\sum_{k_2=21}^{\infty}\exp\left(-\pi^2k^2\alpha\Delta t\right)I_{k_1k_2}\left(t_{f-1}\right)\sin\pi\frac{k_1}{L_x}\xi_1\sin\pi\frac{k_2}{L_y}\xi_2\mid$$

$$\leq\frac{4}{L_xL_y}\sum_{k_1=1}^{p}\sum_{k_2=p+1}^{\infty}\exp\left(-\pi^2k^2\alpha\Delta t\right)\mid I_{k_1k_2}\left(t_{f-1}\right)\mid$$

$$+\frac{4}{L_xL_y}\sum_{k_1=p+1}^{\infty}\sum_{k_2=1}^{\infty}\exp\left(-\pi^2k^2\alpha\Delta t\right)\mid I_{k_1k_2}\left(t_{f-1}\right)\mid \tag{24}$$

Before continuing with the present error analysis, we need to make some useful considerations:

(i)

$$\left(\frac{1-\exp\left(-\pi^2k^2\alpha t\right)}{\pi^2k^2\alpha}\right)\leq\frac{1}{\pi^2k^2\alpha}$$

(ii)

$$\int_0^p\exp\left(-\pi^2\frac{k^2}{L^2}\alpha\delta\right)dk=\frac{L}{\pi\sqrt{\alpha\delta}}\frac{\sqrt{\pi}}{2}\mathrm{erf}\left(\frac{\pi\sqrt{\alpha\delta}p}{L}\right)$$

(iii)

$$\int_p^{\infty}\exp\left(-\pi^2\frac{k^2}{L^2}\alpha\delta\right)dk=\int_0^{\infty}\exp\left(-\pi^2\frac{k^2}{L^2}\alpha\delta\right)dk-\int_0^p\exp\left(-\pi^2\frac{k^2}{L^2}\alpha\delta\right)dk$$

$$=\frac{L\sqrt{\pi}}{2\pi\sqrt{\alpha\delta}}-\frac{L\sqrt{\pi}}{2\pi\sqrt{\alpha\delta}}\mathrm{erf}\left(\frac{\pi\sqrt{\alpha\delta}p}{L}\right)\cong$$

$$\cong\frac{L\sqrt{\pi}}{2\pi\sqrt{\alpha\delta}}-\frac{L\sqrt{\pi}}{2\pi\sqrt{\alpha\delta}}\left(1-\frac{e^{-\pi^2p^2\alpha\delta/L^2}}{\sqrt{\pi}\pi\sqrt{\alpha\delta}\frac{p}{L}}\left[1-\frac{2!}{1!\left(2\pi\sqrt{\alpha\delta}\frac{p}{L}\right)^2}+\frac{4!}{2!\left(2\pi\sqrt{\alpha\delta}\frac{p}{L}\right)^4}-\ldots\right]\right)$$

$$\cong\frac{e^{-\pi^2p^2\alpha\delta/L^2}}{2\pi^2\frac{p}{L^2}\alpha\delta}\left[1-\frac{2!}{1!\left(2\pi\sqrt{\alpha\delta}\frac{p}{L}\right)^2}+\frac{4!}{2!\left(2\pi\sqrt{\alpha\delta}\frac{p}{L}\right)^4}-\ldots\right]$$

$$<\frac{e^{-\pi^2p^2\alpha\delta/L^2}}{2\pi^2\frac{p}{L^2}\alpha\delta}<\frac{e^{-\pi^2p^2\alpha\delta/L^2}}{\pi^2\frac{p}{L^2}\alpha\delta},\qquad\frac{p^2\alpha\delta}{L^2}>0.05$$

(iv)

$$\left| \frac{\partial\left(\sin \pi \frac{k_1}{L_x} x_1 \sin \pi \frac{k_2}{L_y} x_2\right)}{\partial n_{\vec{x}}} \right| \leq$$

$$midgrad\left(\sin \pi \frac{k_1}{L_x} x_1 \sin \pi \frac{k_2}{L_y} x_2\right) \cdot \vec{n}_{\vec{x}} \mid \leq$$

$$\left| \pi \frac{k_1}{L_x} \cos \pi \frac{k_1}{L_x} x_1 \sin \pi \frac{k_2}{L_y} x_2, \pi \frac{k_2}{L_y} \sin \pi \frac{k_1}{L_x} x_1 \cos \pi \frac{k_2}{L_y} x_2 \right| \cdot \left| \vec{n}_{\vec{x}} \right| \leq$$

$$\leq \pi \sqrt{\frac{k_1^2}{L_x^2} + \frac{k_2^2}{L_y^2}}$$

Coming back to the calculation of the truncation error, we can estimate the following bound of the Fourier coefficients:

$$\left| I_{k_1 k_2}\left(t_{f-1}\right) \right| = \alpha \left| \int_0^{t_{f-1}} e^{-\pi^2 \alpha \left(\frac{k_1^2}{L_x^2} + \frac{k_2^2}{L_y^2}\right)\left(t_{f-1} - t\right)} \left(q_{k_1 k_2}(t) - u_{k_1 k_2}(t)\right) dt \right|$$

$$\leq \frac{\left(1 - e^{-\pi^2 \alpha \left(\frac{k_1^2}{L_x^2} + \frac{k_2^2}{L_y^2}\right) t_{f-1}}\right)}{\pi^2 \left(\frac{k_1^2}{L_x^2} + \frac{k_2^2}{L_y^2}\right)} \left\{ \begin{array}{l} \displaystyle\int_\Gamma \left| \frac{\partial\left(\sin \pi \frac{k_1}{L_x} x_1 \sin \pi \frac{k_2}{L_y} x_2\right)}{\partial n_{\vec{x}}} \right| \cdot \max_{0 \leq t \leq t_f} \left| u(\vec{x}, t) \right| d\Gamma_{\vec{x}} \\ + \displaystyle\int_\Gamma \left| \sin \pi \frac{k_1}{L_x} x_1 \sin \pi \frac{k_2}{L_y} x_2 \right| \cdot \max_{0 \leq t \leq t_f} \left| q(\vec{x}, t) \right| d\Gamma_{\vec{x}} \end{array} \right\}$$

$$\leq \frac{1}{\left(\frac{k_1^2}{L_x^2} + \frac{k_2^2}{L_y^2}\right)} |\Gamma| \left\{ \begin{array}{c} \displaystyle\max_{\vec{x} \in \Gamma, 0 \leq t \leq t_{f-1}} \left| u(\vec{x}, t) \right| \pi \left(\frac{k_1^2}{L_x^2} + \frac{k_2^2}{L_y^2}\right)^{1/2} \\ + \displaystyle\max_{\vec{x} \in \Gamma, 0 \leq t \leq t_{f-1}} \left| q(\vec{x}, t) \right| \end{array} \right\}$$

where $|\Gamma|$ is the length of the curve Γ.

As the box is square $L_x = L_y$ then

$$\begin{aligned} \left| I_{k_1 k_2}\left(t_{f-1}\right) \right| &\leq L_x^2 |\Gamma| \left\{ \begin{array}{c} \displaystyle\max_{\vec{x} \in \Gamma, 0 \leq t \leq t_{f-1}} \left| u(\vec{x}, t) \right| \frac{\pi}{L_x} \frac{1}{\left(k_1^2 + k_2^2\right)^{1/2}} + \\ \displaystyle\max_{\vec{x} \in \Gamma, 0 \leq t \leq t_{f-1}} \left| q(\vec{x}, t) \right| \frac{1}{\left(k_1^2 + k_2^2\right)} \end{array} \right\} \\ &\leq L_x^2 |\Gamma| \left\{ \frac{\pi}{L_x} \max_{\vec{x} \in \Gamma, 0 \leq t \leq t_{f-1}} \left| u(\vec{x}, t) \right| + \max_{\vec{x} \in \Gamma, 0 \leq t \leq t_{f-1}} \left| q(\vec{x}, t) \right| \right\} \end{aligned} \tag{25}$$

Using the above bound, the estimation (24) can be written as:

$$
\begin{aligned}
|E_p| &\le \frac{4}{L_x L_y}\sum_{k_1=1}^{p}\sum_{k_2=p+1}^{\infty}\exp\left(-\pi^2 k^2\alpha\Delta t\right)\,|\,I_{k_1k_2}\left(t_{f-1}\right)\,| \\
&\quad + \frac{4}{L_x L_y}\sum_{k_1=p+1}^{p}\sum_{k_2=1}^{\infty}\exp\left(-\pi^2 k^2\alpha\Delta t\right)\,|\,I_{k_1k_2}\left(t_{f-1}\right)\,| \\
&\le \sum_{k_1=1}^{p}\sum_{k_2=p+1}^{\infty}\exp\left(-\pi^2 k^2\alpha\Delta t\right)4\,|\,\Gamma\,|\left\{\frac{\pi}{L_x}\max_{\vec{x}\in\Gamma,0\le t\le t_{f-1}}|\,u(\vec{x},t)\,| + \max_{\vec{x}\in\Gamma,0\le t\le t_{f-1}}|\,q(\vec{x},t)\,|\right\} \\
&\quad + \sum_{k_1=p+1}^{p}\sum_{k_2=1}^{\infty}\exp\left(-\pi^2 k^2\alpha\Delta t\right)4\,|\,\Gamma\,|\left\{\frac{\pi}{L_x}\max_{\vec{x}\in\Gamma,0\le t\le t_{f-1}}|\,u(\vec{x},t)\,| + \max_{\vec{x}\in\Gamma,0\le t\le t_{f-1}}|\,q(\vec{x},t)\,|\right\} \\
&\le 4\,|\,\Gamma\,|\left\{\frac{\pi}{L_x}\max_{\vec{x}\in\Gamma,0\le t\le t_{f-1}}|\,u(\vec{x},t)\,| + \max_{\vec{x}\in\Gamma,0\le t\le t_{f-1}}|\,q(\vec{x},t)\,|\right\}\cdot \\
&\quad \left[\int_0^{p}\exp\left(-\pi^2\frac{k_1^2}{L_x^2}\alpha\Delta t\right)dk_1\int_{p}^{\infty}\exp\left(-\pi^2\frac{k_2^2}{L_y^2}\alpha\Delta t\right)dk_2\right. \\
&\quad \left. + \int_{p}^{\infty}\exp\left(-\pi^2\frac{k_1^2}{L_x^2}\alpha\Delta t\right)dk_1\int_0^{\infty}\exp\left(-\pi^2\frac{k_2^2}{L_y^2}\alpha\Delta t\right)dk_2\right] \\
&\le 4\,|\,\Gamma\,|\left\{\frac{\pi}{L_x}\max_{\vec{x}\in\Gamma,0\le t\le t_{f-1}}|\,u(\vec{x},t)\,| + \max_{\vec{x}\in\Gamma,0\le t\le t_{f-1}}\max|\,q(\vec{x},t)\,|\right\}\cdot \\
&\quad \frac{\exp\left(-\pi^2\frac{p^2}{L_x^2}\alpha\Delta t\right)}{2\pi^3\frac{p}{L_x^2}\alpha\Delta t}\left[\frac{L_x\sqrt{\pi}}{\sqrt{\alpha\Delta t}}\mathrm{erf}\left(\frac{\pi\sqrt{\alpha\Delta t}p}{L_x}\right) + \frac{L_x\sqrt{\pi}}{\sqrt{\alpha\Delta t}}\right] \\
&\le 4\,|\,\Gamma\,|\left\{\frac{\pi}{L_x}\max_{\vec{x}\in\Gamma,0\le t\le t_{f-1}}|\,u(\vec{x},t)\,| + \max_{\vec{x}\in\Gamma,0\le t\le t_{f-1}}|\,q(\vec{x},t)\,|\right\}\cdot \\
&\quad \frac{\exp\left(-\pi^2\frac{p^2}{L_x^2}\alpha\Delta t\right)}{\pi^{\frac{5}{2}}\frac{p}{L_x^2}(\alpha\Delta t)^{\frac{3}{2}}}
\end{aligned}
\tag{26}
$$

Therefore, from the previous calculations it can be seen that the order of the truncation error is $O\left(\frac{\exp -p^2}{p}\right)$.

Appendix 2

In order to calculate the value of $u_{k_1k_2}$ and $q_{k_1k_2}$,i.e.

$$
u_{k_1k_2}(t) = \int_\Gamma \frac{\partial\left(\sin\pi\frac{k_1}{L_x}x_1\sin\pi\frac{k_2}{L_y}x_2\right)}{\partial n_{\vec{x}}}u(\vec{x},t)d\Gamma_{\vec{x}}
$$

and

$$
q_{k_1k_2}(t) = \int_\Gamma \sin\pi\frac{k_1}{L_x}x_1\sin\pi\frac{k_2}{L_y}x_2 q(\vec{x},t)d\Gamma_{\vec{x}}
$$

we consider that u and q vary linearly over each straight-line element Γ_j, where Γ_j is the $j-th$ partition of Γ:

$$u_{k_1k_2}(t) = \int_{\Gamma} \frac{\partial\left(\sin\pi\frac{k_1}{L_x}x_1 \sin\pi\frac{k_2}{L_y}x_2\right)}{\partial n_{\vec{x}}} u(\vec{x},t)d\Gamma_{\vec{x}}$$

$$\cong \sum_{j=1}^{N}\int_{\Gamma_j} \frac{\partial\left(\sin\pi\frac{k_1}{L_x}x_1 \sin\pi\frac{k_2}{L_y}x_2\right)}{\partial n_{\vec{x}}} u(\vec{x},t)d\Gamma_{j\vec{x}}$$

$$\cong \sum_{j=1}^{N} u_j(t)F_j^1(x_1,x_2) - u_{j+1}(t)F_j^2(x_1,x_2)$$

where

$$F_j^1(x_1,x_2) = \frac{1}{2}\left[\frac{\frac{k_2}{L_y}\left(x_1^{j+1}-x_1^j\right) - \frac{k_1}{L_x}\left(x_2^{j+1}-x_2^j\right)}{\frac{k_1}{L_x}\left(x_1^{j+1}-x_1^j\right) + \frac{k_2}{L_y}\left(x_2^{j+1}-x_2^j\right)}\right]\cdot$$

$$\left\{\cos\pi\left[\frac{k_1}{L_x}x_1^j + \frac{k_2}{L_y}x_2^j\right] - \frac{1}{\pi}\left[\frac{\sin\pi\left[\frac{k_1}{L_x}x_1^{j+1} + \frac{k_2}{L_y}x_2^{j+1}\right] - \sin\pi\left[\frac{k_1}{L_x}x_1^j + \frac{k_2}{L_y}x_2^j\right]}{\frac{k_1}{L_x}\left(x_1^{j+1}-x_1^j\right) + \frac{k_2}{L_y}\left(x_2^{j+1}-x_2^j\right)}\right]\right\}$$

$$-\frac{1}{2}\left[\frac{\frac{k_1}{L_x}\left(x_2^{j+1}-x_2^j\right) + \frac{k_2}{L_y}\left(x_1^{j+1}-x_1^j\right)}{\frac{k_2}{L_y}\left(x_2^{j+1}-x_2^j\right) - \frac{k_1}{L_x}\left(x_1^{j+1}-x_1^j\right)}\right]$$

$$\left\{\cos\pi\left[\frac{k_2}{L_y}x_2^j - \frac{k_1}{L_x}x_1^j\right] - \frac{1}{\pi}\left[\frac{\sin\pi\left[\frac{k_2}{L_y}x_2^{j+1} - \frac{k_1}{L_x}x_1^{j+1}\right] - \sin\pi\left[\frac{k_2}{L_y}x_2^j - \frac{k_1}{L_x}x_1^j\right]}{\frac{k_2}{L_y}\left(x_2^{j+1}-x_2^j\right) - \frac{k_1}{L_x}\left(x_1^{j+1}-x_1^j\right)}\right]\right\}$$

and

$$F_j^2(x_1,x_2) = \frac{1}{2}\left[\frac{\frac{k_2}{L_y}\left(x_1^{j+1}-x_1^j\right) - \frac{k_1}{L_x}\left(x_2^{j+1}-x_2^j\right)}{\frac{k_1}{L_x}\left(x_1^{j+1}-x_1^j\right) + \frac{k_2}{L_y}\left(x_2^{j+1}-x_2^j\right)}\right]\cdot$$

$$\left\{\cos\pi\left[\frac{k_1}{L_x}x_1^{j+1} + \frac{k_2}{L_y}x_2^{j+1}\right] - \frac{1}{\pi}\left[\frac{\sin\pi\left[\frac{k_1}{L_x}x_1^{j+1} + \frac{k_2}{L_y}x_2^{j+1}\right] - \sin\pi\left[\frac{k_1}{L_x}x_1^j + \frac{k_2}{L_y}x_2^j\right]}{\frac{k_1}{L_x}\left(x_1^{j+1}-x_1^j\right) + \frac{k_2}{L_y}\left(x_2^{j+1}-x_2^j\right)}\right]\right\}$$

$$-\frac{1}{2}\left[\frac{\frac{k_1}{L_x}\left(x_2^{j+1}-x_2^j\right) + \frac{k_2}{L_y}\left(x_1^{j+1}-x_1^j\right)}{\frac{k_2}{L_y}\left(x_2^{j+1}-x_2^j\right) - \frac{k_1}{L_x}\left(x_1^{j+1}-x_1^j\right)}\right]\cdot$$

$$\left\{\cos\pi\left[\frac{k_2}{L_y}x_2^{j+1} - \frac{k_1}{L_x}x_1^{j+1}\right] - \frac{1}{\pi}\left[\frac{\sin\pi\left[\frac{k_2}{L_y}x_2^{j+1} - \frac{k_1}{L_x}x_1^{j+1}\right] - \sin\pi\left[\frac{k_2}{L_y}x_2^j - \frac{k_1}{L_x}x_1^j\right]}{\frac{k_2}{L_y}\left(x_2^{j+1}-x_2^j\right) - \frac{k_1}{L_x}\left(x_1^{j+1}-x_1^j\right)}\right]\right\}$$

with $u_{N+1} = u_1, x_i^{N+1} = x_i^1, i = 1,2.$

Analogously

$$q_{k_1k_2}(t) = \int_\Gamma \sin\pi\frac{k_1}{L_x}x_1 \sin\pi\frac{k_2}{L_y}x_2 q(\vec{x},t)d\Gamma_{\vec{x}}$$

$$\cong \sum_{j=1}^{N}\frac{l_j}{8}\left\{q_j(t)G_j^1(x_1,x_2) - q_{j+1}(t)G_j^2(x_1,x_2)\right\}$$

where

$$G_j^1(x_1,x_2) = \frac{4\sin\pi\left[\frac{k_1}{L_x}x_1^j + \frac{k_2}{L_y}x_2^j\right]}{\pi\left[\frac{k_1}{L_x}\left(x_1^{j+1}-x_1^j\right)+\frac{k_2}{L_y}\left(x_2^{j+1}-x_2^j\right)\right]}$$

$$+ 4\frac{\cos\pi\left[\frac{k_1}{L_x}x_1^{j+1} + \frac{k_2}{L_y}x_2^{j+1}\right] - \cos\pi\left[\frac{k_1}{L_x}x_1^j + \frac{k_2}{L_y}x_2^j\right]}{\pi^2\left[\frac{k_1}{L_x}\left(x_1^{j+1}-x_1^j\right)+\frac{k_2}{L_y}\left(x_2^{j+1}-x_2^j\right)\right]^2}$$

$$+ 4\frac{\cos\pi\left[\frac{k_1}{L_x}x_1^j - \frac{k_2}{L_y}x_2^j\right] - \cos\pi\left[\frac{k_1}{L_x}x_1^{j+1} - \frac{k_2}{L_y}x_2^{j+1}\right]}{\pi^2\left[\frac{k_1}{L_x}\left(x_1^{j+1}-x_1^j\right)-\frac{k_2}{L_y}\left(x_2^{j+1}-x_2^j\right)\right]^2}$$

$$- \frac{4\sin\pi\left[\frac{k_1}{L_x}x_1^j - \frac{k_2}{L_y}x_2^j\right]}{\pi\left[\frac{k_1}{L_x}\left(x_1^{j+1}-x_1^j\right)-\frac{k_2}{L_y}\left(x_2^{j+1}-x_2^j\right)\right]}$$

and

$$G_j^2(x_1,x_2) = \frac{4\sin\pi\left[\frac{k_1}{L_x}x_1^{j+1} + \frac{k_2}{L_y}x_2^{j+1}\right]}{\pi\left[\frac{k_1}{L_x}\left(x_1^{j+1}-x_1^j\right)+\frac{k_2}{L_y}\left(x_2^{j+1}-x_2^j\right)\right]}$$

$$+ 4\frac{\cos\pi\left[\frac{k_1}{L_x}x_1^{j+1} + \frac{k_2}{L_y}x_2^{j+1}\right] - \cos\pi\left[\frac{k_1}{L_x}x_1^j + \frac{k_2}{L_y}x_2^j\right]}{\pi^2\left[\frac{k_1}{L_x}\left(x_1^{j+1}-x_1^j\right)+\frac{k_2}{L_y}\left(x_2^{j+1}-x_2^j\right)\right]^2}$$

$$+ 4\frac{\cos\pi\left[\frac{k_1}{L_x}x_1^j - \frac{k_2}{L_y}x_2^j\right] - \cos\pi\left[\frac{k_1}{L_x}x_1^{j+1} - \frac{k_2}{L_y}x_2^{j+1}\right]}{\pi^2\left[\frac{k_1}{L_x}\left(x_1^{j+1}-x_1^j\right)-\frac{k_2}{L_y}\left(x_2^{j+1}-x_2^j\right)\right]^2}$$

$$- \frac{4\sin\pi\left[\frac{k_1}{L_x}x_1^{j+1} - \frac{k_2}{L_y}x_2^{j+1}\right]}{\pi\left[\frac{k_1}{L_x}\left(x_1^{j+1}-x_1^j\right)-\frac{k_2}{L_y}\left(x_2^{j+1}-x_2^j\right)\right]}$$

with $q^{N+1} = q^1$ and $l_j = \sqrt{\left(x_1^{j+1}-x_1^j\right)^2 + \left(x_2^{j+1}-x_2^j\right)^2}$.

Appendix 3

For the numerical solution, the computation of the space integral of the single layer potentia,l when the collocation point coincides with one of the ends of an element, was carried out analytically, i.e. singular integration.

The interpolation functions were taken in the following form:

$$\varphi_1(\xi) = \frac{\xi_{j+1} - \xi}{\xi_{j+1} - \xi_j}, \qquad \varphi_2(\xi) = \frac{\xi - \xi_j}{\xi_{j+1} - \xi_j}, \qquad j = 1, ..., N$$

where ξ_j and ξ_{j+1} are the ends of the $j - th$ boundary element Γ_j, and N is the number of elements and nodes.

Taking into account the previous functions, we calculated:

$$\Phi_{ii}^1(\tau) = \int_{\xi_i}^{\xi_{i+1}} \frac{(\xi_{i+1} - \xi)}{(\xi_{i+1} - \xi_i)} exp\left[\frac{-(\xi - \xi_i)^2}{4\alpha(\Delta t - \tau)}\right] d\Gamma_i$$

$$= \sqrt{\pi\alpha(\Delta t - \tau)} erf\left(\frac{(\xi_{i+1} - \xi_i)}{\sqrt{4\alpha(\Delta t - \tau)}}\right) + \frac{2\alpha(\Delta t - \tau)}{(\xi_{i+1} - \xi_i)}\left\{exp\left[\frac{-(\xi_{i+1} - \xi_i)^2}{4\alpha(\Delta t - \tau)}\right] - 1\right\}$$

and

$$\Phi_{ii}^2(\tau) = \int_{\xi_i}^{\xi_{i+1}} \frac{(\xi - \xi_i)}{(\xi_{i+1} - \xi_i)} exp\left[\frac{-(\xi - \xi_i)^2}{4\alpha(\Delta t - \tau)}\right] d\Gamma_i$$

$$= -\frac{2\alpha(\Delta t - \tau)}{(\xi_{i+1} - \xi_i)}\left\{exp\left[\frac{-(\xi_{i+1} - \xi_i)^2}{4\alpha(\Delta t - \tau)}\right] - 1\right\}$$

for $i = 1, \ldots, N$.